ENHANCING SAFETY ON HORIZONTAL CURVES WITH LIMITED SIGHT DISTANCE: A MULTI-OBJECTIVE OPTIMIZATION FRAMEWORK

ENHANCING SAFETY ON HORIZONTAL CURVES WITH LIMITED SIGHT DISTANCE: A MULTI-OBJECTIVE OPTIMIZATION FRAMEWORK

BY:

MOHAMED KHALIL

A THESIS SUBMITTED TO THE SCHOOL OF GRADUATE STUDIES
IN PARTIAL FULFILLMENT OF THE REQUIREMENTS FOR THE DEGREE
MASTER OF APPLIED SCIENCE
MCMASTER UNIVERSITY
APRIL 2021

McMaster University MASTER OF APPLIED SCIENCE (2019) Hamilton, Ontario, (Civil Engineering)

TITLE: Enhancing Safety on Horizontal Curves with Limited Sight Distance: A Multi-Objective Optimization Framework

AUTHOR: Mohamed Khalil

SUPERVISOR: Dr. Mohamed Hussein

NUMBER OF PAGES: 61

ABSTRACT

This study introduces a multi-objective optimization framework for the re-dimensioning of the cross-section elements of rural horizontal curves with limited sight distance. The optimization aims at minimizing both the risk of collision associated with the limited sight distance and the expected collision frequency corresponding to the cross-section elements' dimensions. The risk component was assessed using an index known as (P_{nc}), which is developed based on the reliability theory. The change in collision frequency corresponding to the change of the cross-section elements was extracted from the literature. The risk and the safety components were then combined into one measure ($CMF_{combined}$) to develop a direct measure of the safety impacts of the optimization. The proposed framework was applied to five restricted curves in British Columbia, Canada, considering various scenarios. The results showed a considerable reduction in the P_{nc} value (ranging from 12% to 73%) and the expected collision frequency (ranging from 10% to 31%) after optimization. The estimated combined reduction in collision frequency ($CMF_{combined}$) was estimated to vary between 48% and 76%. The results showed that the optimization of cross-section elements can improve the safety of horizontal curves significantly. The framework presented in this study would support transportation engineers in selecting optimal dimensions of cross-section elements of restricted horizontal curves, understanding the safety consequences of selecting a specific cross-section configuration, and assessing the economic viability of different design options.

PREFACE

This thesis follows the sandwich thesis format of the School of Graduate Studies at McMaster University and includes on submitted paper as follows:

Khalil, M. and Hussein, M. "Enhancing Safety on Horizontal Curves with Limited Sight Distance: A Multi-Objective Optimization Framework", submitted to Journal of Transportation Safety & Security. The submitted paper is presented in chapter 2 of the thesis. The research was started in September 2019 and the manuscript was submitted in April 2021. The research was conducted under the supervision of Dr. Mohamed Hussein. My contributions to the paper are summarized as follows:

- Conducting the Literature review.
- Data collection and processing.
- Optimization Model development.
- Results discussion and interpretation
- Development of the manuscript of the paper.

The co-author contributions include:

- Conceptual design and structure.
- Supervision and technical advice.
- Manuscript review, edit, and development.
- Financial support of the research.

ACKNOWLEDGEMENT

I would like to express my gratitude to Dr Mohamed Hussein for his patience and continuous support. I would like to thank him for the personal and technical advice, and it was a great honour to work under his supervision. I would like to thank the rest of the members of my examination committee, Dr. Wael El-Dakhakhni, Dr. Saiedeh Razavi, and Dr. Zoe Li for their time.

CO-AUTHORSHIP

This research presents analytical work carried out solely by Mohamed Khalil. Advice and guidance were provided for the whole thesis by the academic supervisor Dr Mohamed Hussein. Information presented from outside sources, which has been used towards analysis or discussion, has been cited where appropriate; all other materials are the sole work of the author.

CONTENTS

TABLES

FIGURES

LIST OF ABBREVIATIONS

ASD	Available Sight Distance.
a	Deceleration rate.
B/C	Benefit over Cost ratio.

CMF	Crash Modification Factor.
$CMF_{combined}$	Combined Crash Modification Factor.
CMF_{lane}	Crash Modification Factor for lane width.
$CMF_{shoulder}$	Crash Modification Factor for shoulder width.
CMF_{median}	Crash Modification Factor for median width.
$CMF_{total\text{-}I}(X_j)$	The crash modification factor corresponding to the dimensions of the inner carriageway cross-section elements.
$CMF_{total\text{-}O}(X_j)$	The crash modification factor corresponding to the dimensions of the outer carriageway cross-section elements.
CR	Collision Reduction.
FORM	First-Order Reliability Method.
G	Longitudinal grade.
g	Limit state function.
i	The discount rate.
M	Middle ordinate distance.
M_I	Middle ordinate distance of the inner carriageway.
M_O	Middle ordinate distance of the outer carriageway.
n	Number of years.
P_{nc}	Probability of non-compliance.
$P_{nc\text{-}I}(X_j)$	The probability of non-compliance of the inner carriageway.
$P_{nc\text{-}O}(X_j)$	The probability of non-compliance of the outer carriageway.
PW	Present Worth Value.
PRT	perception and brake reaction time in seconds.
ROW	Right of Way.
R	Horizontal curve radius.
$R_{existing}$	Existing curve radius.

R_{AASHTO}	The standard curve radius recommended by AASHTO.
SPF	Safety Performance Function.
SPWF	Series Present Worth Factor.
SSD	Stopping Sight Distance.
V	Vehicle speed.
V_{design}	Highway design speed.
$V_{operating}$	Vehicle's operating speed.
β	Reliability Index.

CHAPTER 1: INTRODUCTION

The main purpose of road design is to assure safety for motorized and non-motorized road users. While it is widely acclaimed that following the design standards (e.g., AASHTO, TAC) provides safe roads, several studies argued that roads designed according to the existing design guides are not guaranteed to be ultimately safe (e.g., (Hauer, 1999)). The vast majority of geometric design guides were not designed based on explicit safety measures. Rather the geometric design standards were developed based on a conjecture of the reason for the crash occurrence not based on actual knowledge of the cause of the crash. For example, the design of vertical curves was derived based on an assumption that the limited sight distance is the main reason for collision occurrence in the curves. Accordingly, vertical curves are designed to provide adequate sight distance in almost all design guides. Nevertheless, crashes are still occurring in vertical curves that are supposed to be safe according to the design guides. (Hauer, 1999) claimed that deviating from the suggested design values of the geometric design standards can still improve road safety in some cases.

Moreover, the majority of the inputs that are used to design different road elements are stochastic in nature. Considering the design of horizontal curves as an example, curves are typically designed to ensure sufficient superelevation and stopping sight distance for drivers. To achieve that, the designer needs to consider many inputs that varies significantly based on driver and vehicle characteristics and weather conditions, including side friction coefficient, longitudinal friction coefficient, driver deceleration rate, vehicle operating speed, and the perception and reaction time. In order to address the uncertainty of the design inputs, design guides rely on a deterministic approach, in which very conservative estimates of these inputs are used as recommended design inputs. For instance, AASHTO

recommends a design value of 2.5 seconds for the perception and reaction time. Previous studies showed that perception and reaction time actually follows lognormal distribution, with a mean of 1.5s and a standard deviation of 0.4s (Lerner, 1995). This means that the recommended design value by AASHTO is very conservative, as it corresponds to the 99^{th} percentile of the actual distribution of the PRT, which may lead to overdesigned road elements.

The deterministic approach adopted by most design guides was criticized by many studies (e.g., (Ismail, et al., 2009)) due to two main shortcomings: First, the safety margin of the design output in this approach is unknown. Second, in some situations (e.g., roads in restricted environments), the designers may find it difficult to meet the suggested design values due to some budgetary and technical constraints. If the designer needs to deviate from the suggested design values, existing design guides provide little knowledge on the safety implications of such a decision. Currently, the designers do not have a tool that either enables them to compare different alternatives and choose an optimal design option that achieves a balance between safety and construction cost or assess whether the drop in the safety level corresponding to such a deviation from standards is acceptable.

In an attempt to address these issues, probabilistic design approaches that are derived were advocated. Probabilistic design approaches were adopted in the structural engineering field and were incorporated in the structural design guides in the early 1980s ((Ang, et al., 1975) and (Ellingwood, 1980)). In the early stages, a conventional factor of safety was developed by increasing the demand by a multiple of the demand standard deviation and decreasing the supply by a multiple of the supply standard deviation to account for the uncertainties. Later, the reliability theory was advocated to account for the uncertainties associated with the design inputs and developing a safety measure for the design. The safety measure, named the probability of failure, was calculated using the limit state function which presents the difference between the supply and the demand. Given its potential, the application of the reliability analysis in the transportation field was examined in several studies, including for example, (Faghri, et al., 1988), (Richl, et al., 2006), (Sarhan, et al., 2008), and (Ismail, et al., 2010).

The reliability analysis addressed the uncertainties in the design inputs by using a distribution for the random design inputs rather than the single deterministic values suggested by design standards. Besides considering the uncertainties of the random design inputs, the reliability analysis provides a risk measure named probability of failure (probability of non-compliance (P_{nc})). The probability of non-compliance presents the probability of the demand exceeds the supply where a risk of non-compliance will occur. The reliability analysis was widely applied in several

transportation applications such as rail-highway grade crossing, horizontal and vertical curves design, signal design, and calibrating existing guidelines design charts ((Faghri, et al., 1988); (Easa, et al., 2013); (Essa, et al., 2016); (Guo, et al., 2012); (Hussein, et al., 2014); (Hussain, et al., 2016); (Ismail, et al., 2010); (Ismail, et al., 2012); (Jovanovic´, et al., 2011); (Richl, et al., 2006); (Wang, et al., 2017); (Wood, et al., 2014); (Yue, et al., 2020)).

The design of a horizontal curve in mountainous terrain is challenging, especially in highways where median and roadside barriers exist. Meeting the design requirements of minimum curve radius and minimum lateral clearance for sight distance requirements is typically challenging and costly. In such environments, it is extremely difficult to cut through the mountainous terrain to increase the curve radius or expand the ROW to relax the sight distance restrictions. (Ismail, et al., 2012) and (Ibrahim, et al., 2012) proposed a framework for the re-dimensioning of the cross-section of curves with limited sight distance in such environments in order to increase the lateral clearance while maintaining the Right of Way (ROW) and the curve radius unchanged. This study presented in this thesis builds upon the framework proposed in (Ismail, et al., 2012) and (Ibrahim, et al., 2012), addresses the limitations of the two studies, and provides a comprehensive discussion regarding the practical applications of the proposed methodology. Specifically, the study provides a framework to select the optimum combination of different cross-section elements (lane width, shoulder width, median width) for horizontal curves with limited sight distance, using a multi-objective optimization algorithm. The objectives of the optimization are minimizing the risk associated with the limited sight distance, minimizing the expected collision frequency in the curve, and ensuring a balanced risk between the two directions of the highway. The proposed optimization was applied on five tight curves located in the Sea-To-Sky Highway in British Columbia. Three cases were considered in the analysis: 1) existing radius and right of way were maintained unchanged and only the widths of different cross-section elements were allowed to change; 2) The optimal dimensions of the different cross-section elements were obtained for the curve radius required by the AASHTO design guide to evaluate the benefit of the optimization if the minimum curve radius requirements can be fulfilled; and 3) a generalized scenario was considered, in which the optimal cross-section elements were obtained for a wide range of curve radii and ROWs values. The goal of this scenario is to provide a tool that is capable of assessing the safety benefits of different design alternatives and consequently, enables to conduct Cost-Benefit analysis for different design alternatives, in which the additional cost of increasing radius and/or ROW can be compared to the savings resulting from reducing the expected collision frequency. The study provides an example of a Cost-Benefit analysis that was

conducted on one of the curves. The study also provides practical curves, in which designers can select the most economic curve radius and ROW, based on the frequency and severity of collisions observed on the curve.

The thesis is organized as follows: Chapter 1 provides an introduction to the thesis. Chapter 2 represents the main body of the thesis, as it presents the technical paper that summarizes the details of the study. The paper title is "Enhancing Safety on Horizontal Curves with Limited Sight Distance: A Multi-Objective Optimization Framework". Chapter 3 addresses the conclusion and the practical implications of the study. Appendices A_1 and A_2 demonstrate a sensitivity analysis and some generalized models for all curves under investigation, to complement the example presented in chapter 2, which addresses one of the curves only.

CHAPTER 2: ENHANCING SAFETY ON HORIZONTAL CURVES WITH LIMITED SIGHT DISTANCE: A MULTI-OBJECTIVE OPTIMIZATION FRAMEWORK

Abstract: This study introduces a multi-objective optimization framework for the re-dimensioning of the cross-section elements of rural horizontal curves with limited sight distance. The optimization aims at minimizing both the risk of collision associated with the limited sight distance and the expected collision frequency corresponding to the cross-section elements' dimensions. The risk component was assessed using an index known as (P_{nc}), which is developed based on the reliability theory. The change in collision frequency corresponding to the change of the cross-section elements was extracted from the literature. The risk and the safety components were then combined into one measure ($CMF_{combined}$) to develop a direct measure of the safety impacts of the optimization. The proposed framework was applied to five restricted curves in British Columbia, Canada, considering various scenarios. The results showed a considerable reduction in the P_{nc} value (ranging from 12% to 73%) and the expected collision frequency (ranging from 10% to 31%) after optimization. The estimated combined reduction in collision frequency ($CMF_{combined}$) was estimated to vary between 48% and 76%. The results showed that the optimization of cross-section elements can improve the safety of horizontal curves. The framework presented in this study would support transportation engineers in selecting optimal dimensions of cross-section elements of restricted horizontal curves, understanding the safety consequences of selecting a specific cross-section configuration, and assessing the economic viability of different design options.

Keywords: Horizontal curves with limited sight distance, risk of collision, crash modification factors, multi-objective optimization, re-dimensioning of cross-section elements, reliability analysis.

Introduction

According to the United Nations (UN), more than 1.35 million lives are lost every year due to road collisions, making road collisions the 8th leading cause of death worldwide (World Health Organization, 2018). In addition to the tragic loss of human lives, the economic burden of road collisions cannot be underestimated. Jacobs et al., estimated the global annual cost of road traffic injuries to be 518 billion USD (approximately, 1113 billion 2020 USD) (Jacobs, et al., 2000). Highways and rural roads usually witness higher rates of severe and fatal collisions, despite their lower crash frequencies compared to urban roads (Eiksund, 2009) and (Jones, et al., 2008).

Historically, different highway elements are usually designed following the recommendations of some guidelines (e.g., AASHTO, TAC) that are developed to ensure highway safety. Nevertheless, most design guidelines were not developed based on an explicit measure of safety (Hauer, 1999). (Hauer, 1999) argued that roads designed according to the existing design guides are not guaranteed to be ultimately safe and deviating from the design values suggested by the design guides can still improve road safety in some cases.

The majority of existing guidelines rely on a deterministic design approach, in which a singular design value is recommended for the design inputs that are stochastic in nature, such as perception and brake reaction time and deceleration rate. Ismail et al. discussed two main shortcomings of the deterministic approach adopted by existing design guides (Ismail, et al., 2009). First, the deterministic values of the design inputs are often selected very conservatively near the worst-case scenario to address the high degree of uncertainty associated with the design inputs. In some cases, the conservative deterministic approach may lead to over-designed road segments. Second, design guides do not provide a mechanism to assess the safety consequences of deviating from the design standards. According to the current design approaches, any deviation from the design standards, either a small or a large one, is equally unacceptable and unsafe. The aforementioned two issues are specifically significant for roads located in restricted environments, such as mountainous areas. In such environments, the designer may find it difficult to satisfy the guideline requirements for some road segments, mainly due to budgetary and technical constraints. In this case, the designer does not have a reliable tool to determine the impact of any different design on collision frequency and to justify the trade-off between cost and safety. Moreover, since the safety consequences of the design output are unknown, the designer is not often capable of evaluating different design alternatives to select an optimal option based on safety and construction cost.

Reliability analysis has been advocated as a robust approach that is capable of mitigating the above-mentioned shortcomings of the deterministic design approach. Reliability-based design accounts for the uncertainty of the design parameters, as it considers the entire distribution of the design inputs instead of a single recommended value for each input. The Reliability-based design enables to assess the risk associated with each design, through the development of a risk factor, known as the probability of non-compliance (P_{nc}). P_{nc} represents the probability that the demand for a certain feature (e.g., stopping sight distance) exceeds the supply provided by the different road elements. This means that reliability theory provides a powerful tool for assessing the consequences of specific design (in terms of the P_{nc}) and evaluate different design alternatives. To date, the reliability theory has been applied to address various transportation applications, including design of horizontal and vertical curves, investigating pedestrian crossing behaviour and safety, signal design, and calibrating existing guidelines design charts, among other applications (Easa, et al., 2013); (Essa, et al., 2016); (Guo, et al., 2012); (Hussein, et al., 2014); (Hussain, et al., 2016); (Ismail, et al., 2010); (Ismail, et al., 2012); (Jovanovic´, et al., 2011); (Richl, et al., 2006); (Wang, et al., 2017) (Wood, et al., 2014) (Yue, et al., 2020).

This study utilizes the reliability theory to address an important application in highway engineering, namely, the optimization of the cross-section elements to enhance highway safety in restricted environments. The optimization of the highway cross-sections, through the re-dimensioning of cross-section elements, was proposed as a potential solution to enhance vision at horizontal curves with insufficient sight distance in two highways in British Columbia, Canada (Ismail, et al., 2012); (Ibrahim, et al., 2012). The current study introduces a multi-objective optimization framework to select an optimal cross-section for horizontal curves with limited sight distance. The optimization aims at determining an optimal combination of different cross-section elements that minimize the risk associated with the limited sight distance (P_{nc}) and minimizes the expected collision frequency associated with the proposed cross-section while maintaining the same Right of Way (ROW). The concept was applied on five restricted horizontal curves, located along the Sea-to-Sky Highway in southern British Columbia, Canada. Due to the highway topography, the five curves are not satisfying the minimum radius and the sight distance requirements recommended by the design guidelines. First, the optimal cross-sections of the five curves were determined based on the existing curve conditions in order to determine the safety benefits of the optimization in such restricted environments. Second, the optimization was applied to address a hypothetical scenario, in which the curve radii were assumed to satisfy the guideline requirements while the existing ROW was maintained. The goal is to investigate the safety benefits of the cross-

section optimization in cases where only sight distance requirements are not satisfied and assess whether the additional cost, resulted from increasing the curve radii, can be justified by the reduction in collision cost. Finally, a more general case was considered, in which the optimization was applied to determine the optimal cross-sections for a combination of different curve radii and ROWs. The goal is to assess the safety benefits corresponding to the different curve radii and ROWs combinations, which facilitates conducting Cost-Benefit analyses, by comparing the additional construction costs associated with a particular combination with the savings achieved from the collision reduction.

The current study provides several contributions to the literature. First, compared to previous studies that addressed cross-section optimization, this study provides a comprehensive analysis that considers various scenarios of particular interest to designers and planners. Second, the objective function of the optimization algorithm includes components to explicitly assess the change in collision frequency corresponding to the change of different cross-section elements (shoulders, lanes, and median). Third, the study combined the change in the risk factor (P_{nc}) and the expected collision frequency after optimization into one measure ($CMF_{combined}$), which assists designers and road authorities to quantify the safety consequences of the optimization and conduct rapid and accurate C/B analyses. The rest of the paper is organized as follows: Section 2 provides a summary of the literature, section 3 addresses the methodology, section 4 illustrates the case study, section 5 demonstrates the results and discussion, and section 6 provides the conclusion and recommendations for future works.

Literature Review

Reliability analysis has been advocated as an emerging technique that is capable of addressing the inconsistency associated with existing design guides, account for the uncertainty of the design inputs, and quantify the risk corresponding to a particular design. Numerous studies can be found in the literature that applied reliability analysis to address different transportation applications. For example, Ismail et al. applied the reliability theory to evaluate the risk associated with limited sight distance at nine horizontal curves in two different highways in British Columbia, Canada (Ismail, et al., 2010). The study reported high variability in the inherent risk of the different curves despite being designed according to the same standards, which highlighted the issue of the inconsistency of the existing design guides. (Hussein, et al., 2014) proposed an approach to calibrate geometric design standards to yield consistent risks for the design outputs and enable the assessment of the consequences of deviating from design standards. Essa et al. utilized a multi-mode reliability approach (system reliability) to design horizontal curves with limited sight distance

while considering multiple potential modes of noncompliance (sight distance and skidding) (Essa, et al., 2016). The study recommended that future studies should attempt to investigate the re-dimensioning of the cross-section elements of the highway to develop an optimal safety level of the road. (Sarhan, et al., 2008) applied the reliability theory to evaluate the risk associated with inadequate sight distance at horizontal curves. The study was one of the first studies to consider the three-dimensional sight distance requirements as opposed to two-dimensional sight distance. (Hussain, et al., 2016) applied reliability analysis to evaluate the risk associated with the limited sight distance available for left-turn vehicles at signalized intersections with permissive left-turn phases. (Easa, et al., 2013) proposed a probabilistic approach to design the pedestrian walk interval, using the first-order second-moment reliability method (FOSM).

Furthermore, few studies attempted to establish a link between the risk measure (P_{nc}) and an objective safety measure, such as collision frequency, so that the impact of the numerous applications discussed above can be directly translated into tangible safety benefits. Ibrahim et al. established such a link by incorporating the reliability risk measure (P_{nc}) as an independent variable in the safety performance functions (SPF) (Ibrahim, et al., 2011). The study developed SPFs to predict the frequency of the total, severe, and Property Damage Only collisions at 100 horizontal curves along the Trans-Canada Highway in British Columbia. The results showed that the P_{nc} has a direct relationship with the expected collision frequency, with statistically significant parameters calculated in all functions (Ibrahim, et al., 2011).

In addition, previous research addressed the optimization of cross-section elements to achieve higher safety levels and reduces the risk associated with a particular roadway element. (Ismail, et al., 2012). proposed a methodology to optimize the different cross-section elements using a multi-objective optimization algorithm that aims at minimizing the average risk (P_{nc}), ensure the consistency of the average risk between the two directions of the highway, and minimize the collision frequency. The results of the study showed an average reduction in the risk measure (P_{nc}) by 25% after the optimization. However, the change in collision frequency was presented to the optimization model in terms of crash modification factors (CMFs) that were derived from the work of (Harwood, et al., 2003). The CMFs reported in (Harwood, et al., 2003) were developed based on an assumption of an inverse relationship between lane width and collision frequency, which was challenged by several studies later on (e.g., (Hauer, 2000); (Qin, et al., 2004); (Gross, et al., 2011) (Gross, 2013); (Lee, et al., 2015)). As well, a more accurate objective function was needed to express the change in collision frequency associated with the change of each cross-section element (e.g., lane width,

shoulder width, and median width). Ibrahim et al. (Ibrahim, et al., 2012) advanced the work of (Ismail, et al., 2012) by incorporating the P_{nc} in the calculation of the CMFs, using the established relationship between the P_{nc} and the CMF in (Ibrahim, et al., 2011). The updated model outperformed the old model because of the more accurate representation of the CMF. However, the study emphasized the importance of investigating the safety consequences of changing the dimension of each cross-section element separately, which is addressed in this study.

Methodology

This study proposes a multi-objective optimization framework to determine the optimal dimensions of the cross-section elements that yield the minimum risk and the minimum collision frequency. The reliability theory was utilized to calculate the risk associated with the different design options (P_{nc}). Crash modification factors (CMFs) corresponding to different design options were estimated based on the literature and incorporated in the optimization algorithm to account for the safety level of the different cross-sections. The following sections provide a brief description of the reliability theory, the calculation of the risk index of the different design options, and the multi-objective optimization algorithm that is used to calculate the optimal section of the horizontal curves under investigation.

Reliability Analysis

The reliability problem starts with defining a limit state function, which represents the difference between the supply (S) and the demand (D) of the problem under investigation, as shown in Equation 1.

$$g = S - D \quad (1)$$

If the demand exceeds the supply (i.e., g < 0), a failure (non-compliance) is defined. Alfredo et al. (Alfredo, et al., 1979) provides a robust approach to calculate a measure of safety (MS) that accounts for the uncertainty of the demand and the supply variables, named the reliability index (β), and the probability of non-compliance (i.e., the probability that the demand exceeds the supply), as presented in Equations 2-4.

$$MS = E(S) - E(D) \quad (2)$$

$$\beta = \frac{MS}{\sqrt{\sigma^2 S + \sigma^2 D}} \quad (3)$$

$$P_{nc} = \phi(-\beta) \quad (4)$$

Where:

E(S) and E(D) are the expectations of the supply and the demand functions, respectively.

σ^2S and σ^2D are the variances of the supply and the demand functions, respectively.

P_{nc} is the probability of non-compliance.

$\Phi(-\beta)$ is the cumulative distribution function of the $-\beta$ in the standard normal distribution domain.

In the context of horizontal curves with limited sight distance, the supply is represented by the available sight distance (ASD) on the horizontal curves, while the demand is the required stopping sight distance (SDD) by the driver. The available sight distance and the stopping sight distance can be calculated according to AASHTO design guide, as shown in Equations 5 and 6, respectively.

$$ASD = \frac{R}{28.65} \times Cos^{-1}(1 - \frac{M}{R}) \quad (5)$$

$$SSD = 0.278 \times V \times PRT + \frac{0.039V^2}{a+9.81G} \quad (6)$$

Where R is the radius of the centerline of the inner lane, M is the middle ordinate distance (lateral clearance) that is dependent on the dimensions of the different cross-section elements, PRT is the perception and brake reaction time in seconds, V is the vehicle speed in (km/h), a is the deceleration rate in (m/s^2), and G is the longitudinal grade. Accordingly, the limit state function in this study is defined as follows:

$$g = ASD - SSD = \frac{R}{28.65} \times Cos^{-1}\left(1 - \frac{M}{R}\right) - \left[0.278 \times PRT + \frac{0.039V^2}{a+9.81G}\right] \quad (7)$$

Equation 7 includes three stochastic variables that vary significantly among drivers, mainly, the perception and brake reaction time (PRT), the deceleration rate (a), and the vehicle speed (V). The statistical distributions of the three parameters along with the corresponding mean and standard deviation values were obtained from previous studies, as shown in (Table 2.1).

Table 2.1: Probability distribution of the design inputs.

Parameter	Mean	Standard Deviation	Distribution	Source
Perception and Brake Reaction Time (PRT)	1.5s	0.4s	Lognormal	(Lerner, 1995)
Operating Speed (V)	Model*	Model*	Normal	(Richl, et al., 2006)
Deceleration (a)	4.2 m/s^2	0.6 m/s^2	Normal	(Fambro, et al., 1997)

** Refer to Figure 2.1.*

Regarding the operating speed, the mean and the standard deviation of the operating speed corresponding to different curve radii were calculated based on the work of (Richl, et al., 2006), which combined nine operating speed models to develop a comprehensive model for operating speeds on horizontal curves. The mean and the standard deviation corresponding to different curve radii are shown in Figure 2.1.

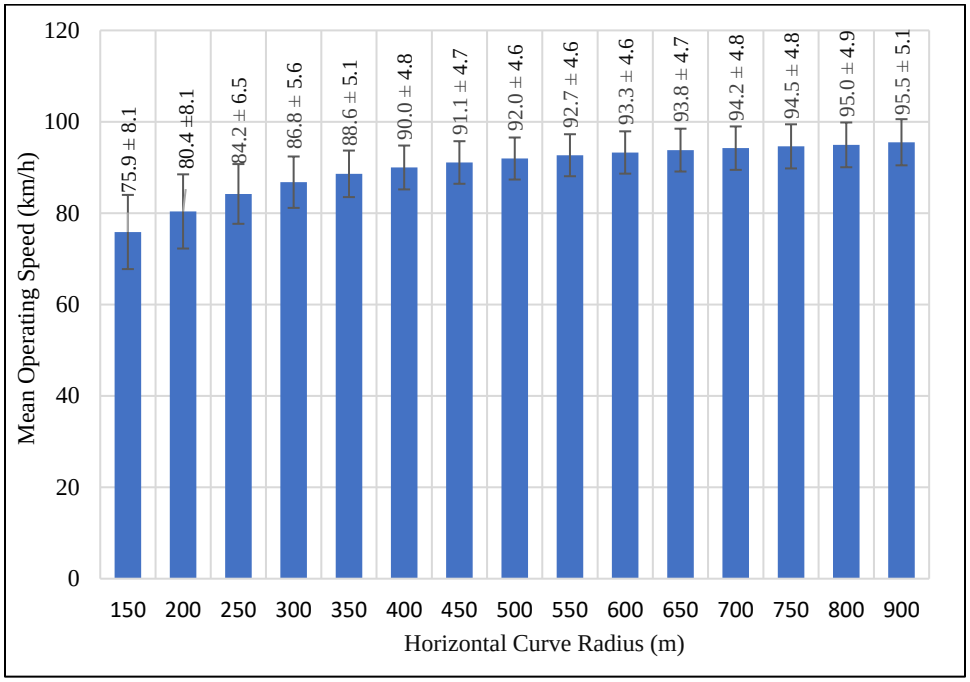

Figure 2.1: Operating speed distribution

In order to solve Equation 7 and calculate the probability of non-compliance, the first-order reliability method (FORM) was utilized. In FORM, the space of random variables is transformed to the standard normal space and the limit state function (g) is linearized near the origin at the so-called design point or the most probable failure point. The reliability index (β) is represented by the distance between the design point and the origin. Subsequently, the P_{nc} can be determined by calculating the cumulative distribution function of (-β) in the standard normal domain. FORM has several merits compared to other reliability methods. The FORM outperforms sampling techniques as it requires a considerably lower number of iterations. Also, FORM considers the distribution of the random variable, not only the mean and the standard deviation. FORM also remedies the invariance problem that occurs in the mean-value first-order second-moment reliability methods. On the other hand, as FORM preserve the linearization of the limit state function, it is considered inaccurate in cases where the limit state function is highly non-linear. In this study, the

FORM algorithm was implemented using Rt software, which was developed by Mashuli et al. at the University of British Columbia in Vancouver, Canada (Mahsuli, et al., 2013).

Cross-Section Re-Dimensioning Using Multi-Objective Optimization

Sharp horizontal curves are challenging sections of highways, due to the sight distance restrictions, especially, if roadside and median barriers are used to mitigate certain types of collisions. Cross-section re-dimensioning shows the potential to improve the available sight distance in such conditions (Ismail, et al., 2012) and (Ibrahim, et al., 2012). Cross-section re-dimensioning aims at changing the dimensions of different cross-section elements, such as lane, shoulder, and median width, to improve the available sight distance on the curve while maintaining the same ROW. Although safety can be enhanced through achieving better sight distance on horizontal curves, changing the dimensions of certain cross-section elements can have a negative impact on safety. As such, the cross-section re-dimensioning can be seen as an optimization problem, in which the designer seeks optimal dimensions for the different cross-section elements to maximize the available sight distance and minimize the negative impact on safety at the same time.

Two different measures were incorporated in the objective function of the optimization problem: First, the probability of non-compliance (P_{nc}), which represents the risk associated with the limited sight distance component of the optimization. A reduction in the P_{nc} indicates that more sight distance becomes available to the driver and consequently, the risk of collision is decreased. Second, the crash modification factor corresponding to the dimensions of the different cross-section elements. As the CMF decreases, the expected collisions on the curve under investigations decrease, and consequently, safety is improved. Based on this, it is desirable to minimize both the probability of non-compliance and the CMF of the roadway. Accordingly, the cross-section re-dimensioning can be expressed according to the following optimization problem:

$$Minimize\ F(X_j) = \alpha_1 \times CMF_{total-I}(X_j) + \alpha_2 \times CMF_{total-O}(X_j) + \alpha_3 \times P_{nc-I}(X_j) + \alpha_4 \times P_{nc-O}(X_j) + \alpha_5 \times \left(1 - \frac{P_{nc-I}(X_j)}{P_{nc-O}(X_j)}\right) \quad (8)$$

Subject to:

$$B_{j(min)} < X_j < B_{j(max)} \quad (9)$$

$$\sum_{j=1}^{j} X_j = ROW \quad (10)$$

$$X_j \geq 0 \qquad (11)$$

Where:

X_j	A vector including all decision variables (cross-section elements).
$CMF_{total\text{-}I}(X_j)$	The crash modification factor corresponding to the dimensions of the inner carriageway cross-section elements.
$CMF_{total\text{-}O}(X_j)$	The crash modification factor corresponding to the dimensions of the outer carriageway cross-section elements.
$P_{nc\text{-}I}(X_j)$	The probability of non-compliance of the inner carriageway.
$P_{nc\text{-}O}(X_j)$	The probability of non-compliance of the outer carriageway.
$\alpha_{1\text{-}5}$	The assigned weights.

The multi-objective function shown in Equation 8 consists of five main components, the first and second components represent the expected change in collision frequency due to the change of the dimensions of the different cross-section elements of the inner and outer carriageways, respectively. The total CMFs in Equation 8 ($CMF_{total\text{-}I}$, $CMF_{total\text{-}O}$) are calculated as the product of the CMFs corresponding to any combination of shoulder, lane, and median widths in each carriageway, as will be explained in detail in the case study section. The third and fourth components represent the probability of non-compliance corresponding to the available sight distance in each of the two carriageways. The fifth component aims at ensuring a balanced risk (P_{nc}) between the inner and the outer carriageways. The decision variable vector (X_j) includes five variables: The inner and the outer shoulder width, the inner and the outer lane width, and the median width. The minimum values of the decision variables considered in the study ($B_{j(min)}$) were 9 ft, 0 ft, and 4.9 ft, for lane, shoulder, and median width, respectively. The maximum values of the decision variables ($B_{j(max)}$) in this study were 13.5 ft, 12 ft, and 30 ft, for lane, shoulder, and median width, respectively. Both P_{nc} and CMF of the inner and outer carriageways are directly related to the decision variables, which means that Equation 8 can be expressed in terms of the five decision variables (X_j) only, as will be shown in the following section. The optimization was conducted using the Generalized Reduced Gradient (GRG) excel solver algorithm.

Equation 8 requires the values of the probability of non-compliance and the collision modification factors of both carriageways to be determined, as functions in the decision variables (widths of the different cross-section elements). To that end, the middle ordinate distances of the inner and outer carriageways corresponding to any cross-

section configuration can be calculated as shown in Equations 12 and 13, respectively. Once the middle ordinate distances are known, the limit state function, expressed in Equation 7, can be analyzed using the FORM algorithm to determine the P_{nc} values of the two carriageways ($P_{nc\text{-}I}$, $P_{nc\text{-}O}$) corresponding to any cross-section configuration, according to the methodology presented in the previous section.

$$M_I = Inner\ Shoulder\ Width + \frac{Inner\ Lane\ Width}{2} \quad (12)$$

$$M_O = \frac{Outer\ Lane\ Width}{2} + (Median\ width - 1\ (meter)) \quad (13)$$

Case Study

The multi-objective optimization was applied to determine the optimal dimensions of the cross-section elements of five horizontal curves along the Sea-to-Sky Highway in British Columbia, Canada. This highway is restricted by a rough mountainous terrain from the east and the water surface of the Howe Sound from the west. The terrain topography makes it extremely costly to increase the radii of the horizontal curves or increase the Right of Way to provide adequate sight distance at horizontal curves. As such, many curves along the road, including the five curves investigated in this study, are very sharp and do not satisfy either the minimum radius or the sight distance requirements. In the early 2000s, median and side barriers were added at the majority of the highway's horizontal curves in order to mitigate the run-off-road and opposite direction collisions, which were very common along the highway. Although the barriers managed to reduce the frequency of run-off-road and opposite direction collisions significantly, they limited the available sight distance at horizontal curves, particularly sharp curves, which increased the risk of collision for other types of crashes such as (e.g., rear-end and fixed object crashes). Given the ROW restriction, the multi-objective optimization was applied to the five curves to investigate the potential safety benefits of the re-dimensioning of the cross-section elements of the five curves. The geometric details of the five curves are shown in Table 2.2, while Figure 2.2 shows their typical cross-section.

Table 2.2: Details of the five horizontal curves

Curve Number	Design Speed	Radius	Lane width	Outer Shoulder Width	Number of Lanes	Median Width	e	G	SSD	Existing M_I, M_o	Standard M (AASHTO)
	(km/h)	(meter)	(meter)	(meter)		(meter)	%	%	(meter)	(meter)	(meter)
1	80	160	3.5	1.5	4	2	6.4	-0.7	129	3.25, 2.75	12.8
2	70	190	3.5	1.5	4	2	5.4	2.6	104	3.25, 2.75	7.2
3	80	190	3.5	1.5	4	2	5.4	-1.2	129	3.25, 2.75	10.8
4	80	210	3.5	1.5	4	2	6.3	3	128	3.25, 2.75	9.8
5	80	220	3.5	1.5	4	2	6.2	5.9	128	3.25, 2.75	9.2

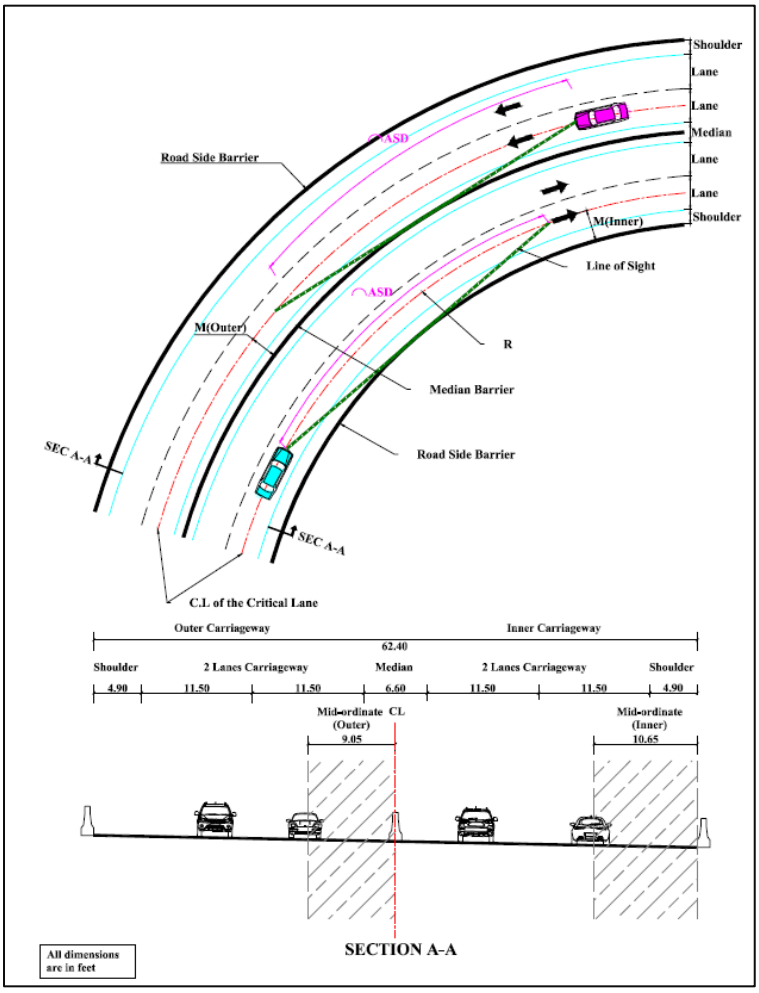

Figure 2.2: Plan and typical cross-section of the five horizontal curves

Four scenarios were considered in the optimization. First, vehicle speeds were assumed to be constant and equal to the design speed of the highway (**Scenario I**). Second, the impact of the variability of vehicle speeds was considered by using the operating speed distribution rather than the design speed (**Scenario II**). Moreover, in order to assess the potential benefit of the cross-section optimization in conditions where only sight distance requirements are not satisfied, two hypothetical scenarios were considered, in which the curve radii were assumed to be equal to the standard radius, resulted from AASHTO design procedures. The idea is to evaluate whether the cross-section optimization is beneficial in cases where curve radius is designed according to the standards or only it can be applied to extreme cases where the designers have to deviate from standard practice. Also, the two scenarios will enable to conduct Cost-Benefit analysis so that the designer can assess whether the collision saving resulting from the cross-section optimization can compensate for the additional cost associated with increasing the curve radius. In (**Scenario III**), the standard radius was considered along with the design speed of the highway. In (**Scenario IV**), the standard radius was considered along with the operating speed of the drivers. In each scenario, the multi-objective optimization (Equation 8) is applied to determine the optimal dimensions of the cross-section elements of each curve. The CMF and the P_{nc} corresponding to the optimal section are then determined in order to assess the safety benefits associated with the proposed section.

It should be noted that the median barrier was always located at 1.0 m from the inner carriageway regardless of the median width resulted from the optimization. The rationale of this decision is that the median barrier only restricts vision on the outer carriageway. As such, an increase in the distance between the median barrier and the outer carriageway will enhance sight distance on the outer carriageway significantly. Regarding the crash modification factors of the inner and the outer carriageways ($CMF_{total\text{-}I}$, $CMF_{total\text{-}O}$) corresponding to any cross-section configuration, they are calculated as the product of the CMFs corresponding to the dimensions of the lane, shoulders, and median, as follows:

$$CMF_{total-I} = (CMF_{lane-I} \times CMF_{shoulder-I} \times CMF_{median-I}) \quad (14)$$

$$CMF_{total-O} = (CMF_{lane-o} \times CMF_{shoulder-O} \times CMF_{median-O}) \quad (15)$$

Where CMF_{lane}, $CMF_{shoulder}$, and CMF_{median} are the crash modification factors corresponding to any lane, shoulder, median width, respectively. In this study, the CMFs corresponding to different lane widths were extracted from the work of Gross (Gross, 2013). The different CMF values corresponding to different lane widths are presented

in Table 2.3 As shown in the table, (Gross, 2013) used the lane width of 12 ft as a reference and reported the CMF corresponding to other lane widths based on the ratio of the collision frequency at each lane width and the collision frequency at the standard lane width (12 ft).

Table 2.3: CMF for different lane widths**

Lane width (Feet)	CMF (per direction)
9	0.90
9.5	0.99
10	1.08
10.5	1.09
11	1.08
11.5	1.09
12	1.00
12.5	0.88
13	0.90
13.5	0.91

** *Calculated based on the work of* (Gross, 2013)

Regarding the shoulder and the median widths, numerous studies observed an inverse relationship between both shoulder and median widths and collision frequency (e.g., (Abdel-Aty, et al., 2014); (Gross, et al., 2007); (Lord, et al., 2008); (Pratt, et al., 2013); (Harkey, 2008); (Stamatiadis, et al., 2009)). The CMFs corresponding to different shoulder widths were extracted from the work of (Gross, et al., 2007) and the Highway safety manual (AASHTO Part D, 2010), as shown in Table 2.4 The CMFs corresponding to different median widths were obtained from the work of (Harkey, 2008), as shown in Table 2.5 It should be noted that The CMFs reported in the previous studies reflects the effect of the cross-section elements (lane, shoulder and median width) on collision frequency for the whole road. Since the CMF_{lane}, $CMF_{shoulder}$, and CMF_{median} are needed per direction, it was assumed that the impact of cross-section elements width on collision frequency is equally distributed across the two directions.

Table 2.4: CMF for different shoulder widths**

Shoulder width (Feet)	CMF (per direction)
0	1.12
1	1.12
2	1.07

Shoulder width (Feet)	CMF (per direction)
3	1.06
4	1.01
5	0.99
6	0.97
7	0.97
8	0.95
9	0.80
10	0.84

** *Calculated based on the work of* (Gross, et al., 2007) *and* (AASHTO Part D, 2010)

Table 2.5: CMF for different median widths**

Median width (Feet)	CMF (per direction)
10	1.00
20	0.96
30	0.93

** *Calculated based on the work of* (Harkey, 2008)

Lastly, the weights of the different components of the multi-objective optimization (Equation 8) were selected based on preliminary sensitivity analysis to test the impact of the weight on the results. Different weight combinations were examined in which the weights of the different components increased and decreased by up to 100%. The results of the sensitivity analysis showed that the maximum change in the P_{nc} and CMF of the resulted optimal section was 10%, which indicated a marginal effect of the assigned weights on the optimization results. As such, the weights of the five components were set equally ($\alpha_{1\text{-}5} = 0.2$).

Results and Discussion

Generally, the results showed a considerable reduction in the inherent risk as well as the collision frequency as a result of the re-dimensioning of the cross-section elements in all scenarios. The cross-section dimensions before and after optimization for the **first scenario** ($R_{existing}$, V_{design}) are shown in Table 2.6.

Table 2.6: Cross-section elements before and after optimization (Scenario I)

Cross-Section Element	Existing Cross-Section (ft)	Dimensions After Optimization (ft)				
		Curve (1)	Curve (2)	Curve (3)	Curve (4)	Curve (5)
Inner carriageway shoulder	4.90	11.60	11.60	11.60	11.60	11.60
Inner carriageway lanes	11.50	9.00	9.00	9.00	9.00	9.00
Outer carriageway shoulder	4.90	0.00	0.00	0.00	0.00	0.00
Outer carriageway Lane	11.50	9.00	9.00	9.00	9.00	9.00
Median	6.60	14.80	14.80	14.80	14.80	14.80
Right of Way	62.40	62.40	62.40	62.40	62.40	62.40

The CMF and the P_{nc} of the five curves after the optimization are shown in Figure 2.3. As shown in the figure, constant CMFs of 0.69 and 0.9 were achieved at the five curves following the re-dimensioning of cross-section elements of the inner and the outer carriageway, respectively. The expected reduction in collision frequency is mainly attributed to the increase in median width and the reduction of lane width in both carriageways. For all curves, the expected collision reduction in the inner carriageway is greater than the outer carriageway. The main reason for such difference is that the optimization resulted in a significant reduction in the outer carriageway shoulder to accommodate an increase in the median width to provide more lateral clearance for the outer carriageways. On the contrary, the shoulder width of the inner carriageway was increased to provide more lateral clearance, as it is directly involved in the lateral clearance of the inner carriageway. Moreover, the results show a considerable reduction in the P_{nc} that ranges from 0.12 and 0.67. The P_{nc} of the inner and the outer carriageways after the optimization ranges from 0.88 for the sharpest curve (Curve 1) and 0.08 for the curve with the closest radius to the standard radius of AASHTO (Curve 2).

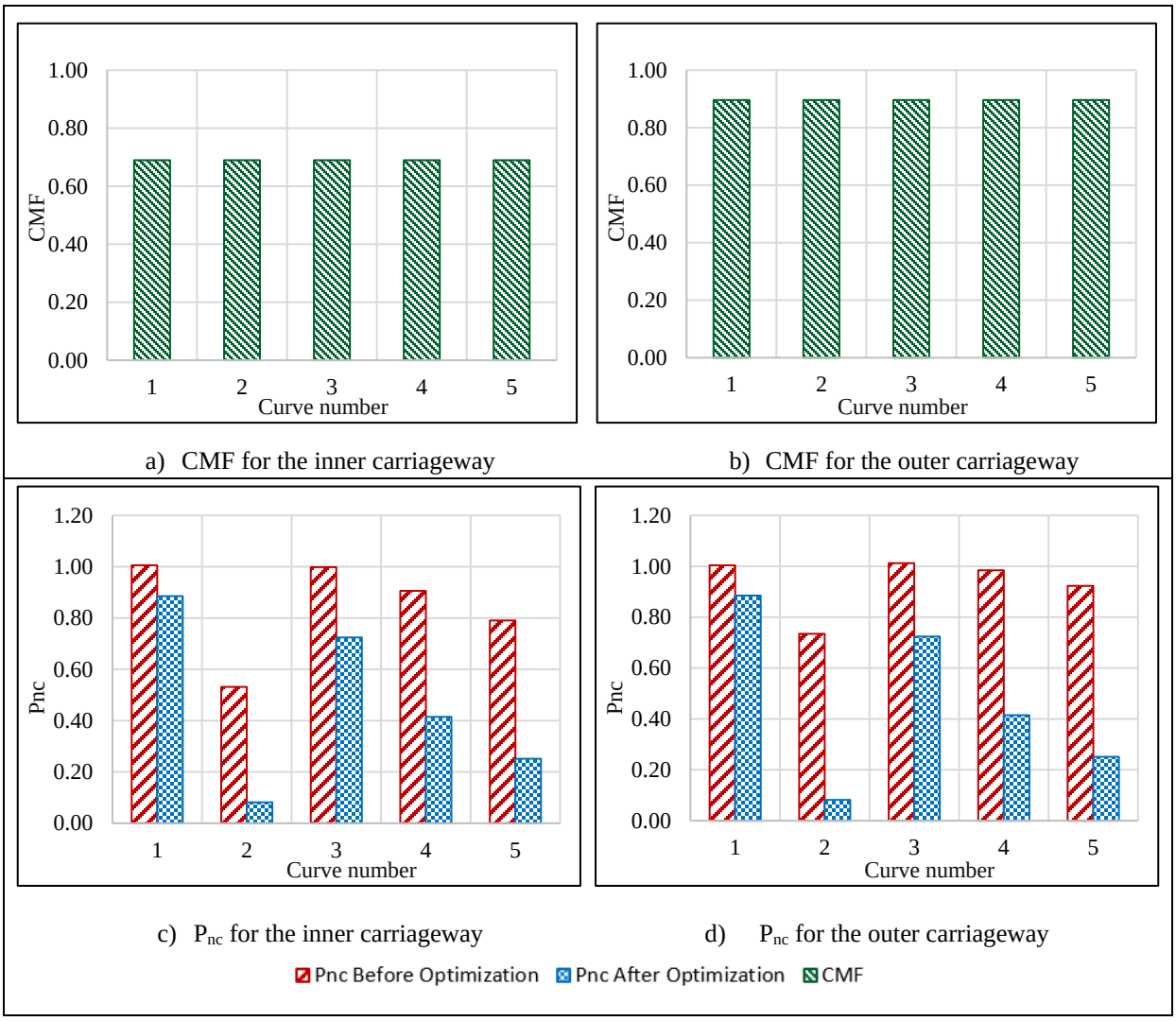

Figure 2.3: CMF and P_{nc} before and after optimization (Scenario I)

In the **second scenario**, the operating speed distribution was considered as opposed to the design speed ($R_{existing}$, $V_{operating}$). The dimensions of the cross-section elements before and after optimization are shown in Table 2.7, while the CMF and the P_{nc} of the five curves after the optimization are shown in Figure 2.4. The results show that the optimal cross-sections and the CMFs of the five curves did not change, compared to the first scenario. However, there is a significant difference in the results of the probability of non-compliance (P_{nc}) between the two scenarios.

As shown in Figure 2.4, the consideration of the operating speed distribution leads to a significantly lower reduction in the P_{nc} after optimization in the second scenario. The reduction in P_{nc} after optimization ranges between 0.24 and 0.46 in Scenario II. Moreover, the variability in the P_{nc} values among curves in the second scenario is much lower than in the first scenario. The P_{nc} values after the optimization range between 0.66 for the sharpest curve (curve

1) and 0.40 for the widest curve (Curve 5). This is mainly because the design speed, which was considered in the first scenario, was almost constant along all the curves, with the exception of the second curve, despite the variability in the curve radii. This leads to significant variability of the risk associated with the limited sight distance among curves. On the contrary, the operating speeds considered in the second scenario are dependent on the curve radii and reflect the actual driver behaviour in selecting the vehicle speed based on their comfort and safety perception. The variation of the values of the P_{nc} between the two scenarios shows the significance of considering the actual speed distribution when conducting the re-dimensioning in order to get a more accurate estimation of the reduction in the risk and the safety enhancement.

Table 2.7: Cross-section elements before and after optimization (Scenario II)

Cross-Section Element	**Existing Cross-Section (ft)**	**Dimensions After Optimization (ft)**				
		Curve (1)	Curve (2)	Curve (3)	Curve (4)	Curve (5)
Inner carriageway shoulder	4.90	11.60	11.60	11.60	11.60	11.60
Inner carriageway lanes	11.50	9.00	9.00	9.00	9.00	9.00
Outer carriageway shoulder	4.90	0.00	0.00	0.00	0.00	0.00
Outer carriageway Lane	11.50	9.00	9.00	9.00	9.00	9.00
Median	6.60	14.80	14.80	14.80	14.80	14.80
Right of Way	62.40	62.40	62.40	62.40	62.40	62.40

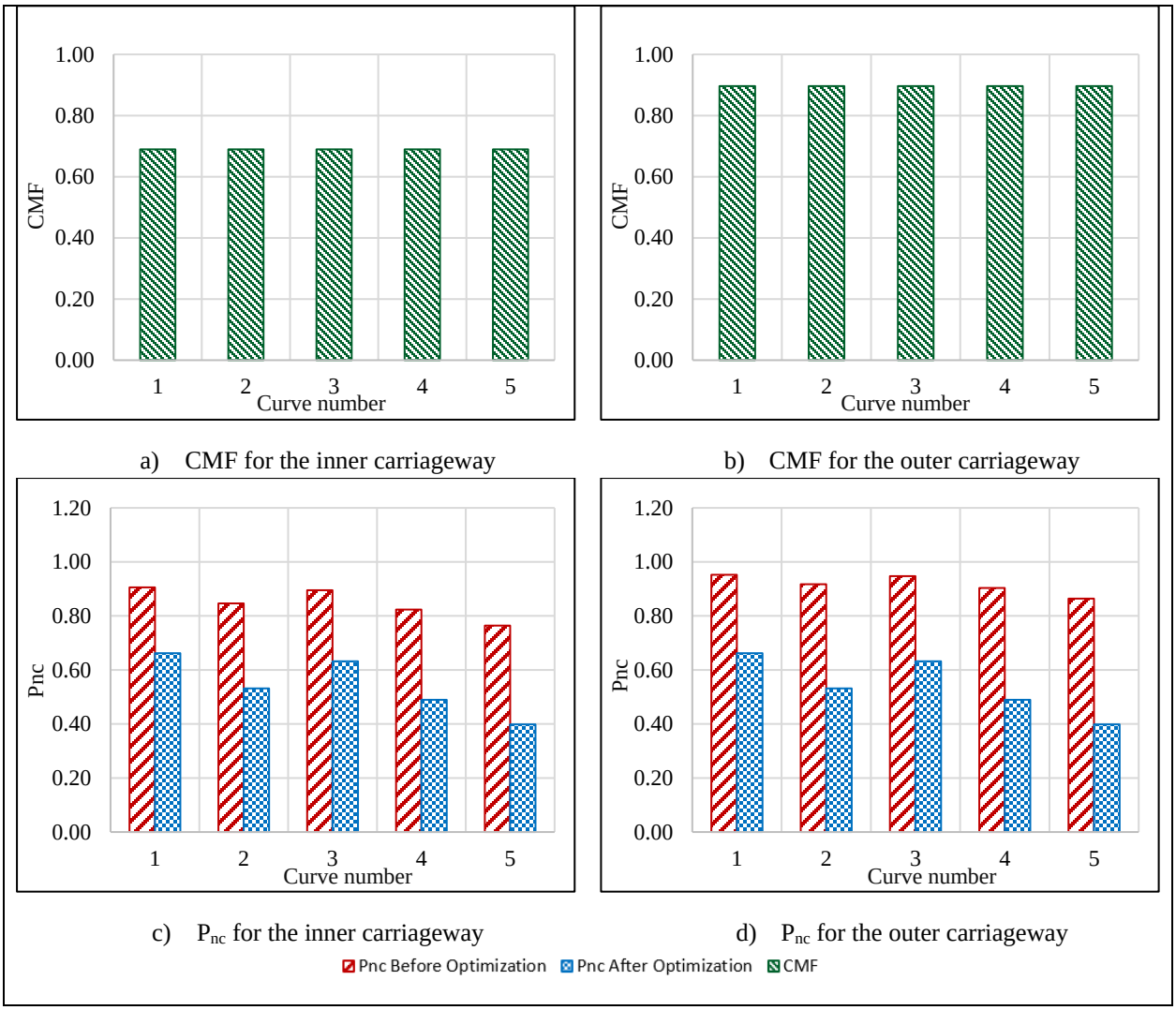

Figure 2.4: CMF and P_{nc} before and after optimization (Scenario II)

In the **third and the fourth scenarios**, the standard curve radii, based on the AASHTO design guidelines, were considered along with the design and operating speeds, respectively. Since the radius of the second curve already meets the AASHTO requirements, the second curve was excluded from the two scenarios. The optimization yields a similar cross-section configuration in both scenarios, as shown in Table 2.8. The corresponding CMFs and P_{nc} values in the two scenarios are shown in Figure 2.5 and Figure 2.6, respectively. The two figures showed consistent CMF among the four curves after the re-dimensioning (0.69 for the inner carriageway and 0.90 for the outer carriageway). The results showed that the increase in curve radii managed to reduce the P_{nc} values before the optimization in all curves; however, the reduction was not significant. For example, the $P_{nc\text{-}I}$ for the first curve before optimization dropped from 1.0 in Scenario I to 0.83 in Scenario III. This was expected since the risk corresponding to limited sight

distance is more dependent on the dimensions of the cross-section elements than it is on the curve radius. The optimization managed to achieve a significant reduction in P_{nc} values in the two scenarios among all curves. Figure 2.5 shows a reduction in the P_{nc} among the four curves that ranges between 0.51 to 0.73 in the third scenario (V_{design}, R_{AASHTO}), while Figure 2.6 shows a reduction ranging between 0.33 to 0.56 for the fourth scenario ($V_{operating}$, R_{AASHTO}). The results of Scenario III and Scenario IV showed the substantial safety benefits of the cross-section optimization, even if the curve radii satisfy the requirements of the design guidelines.

Table 2.8: Cross-section elements before and after optimization (Scenario III and IV)

Cross-Section Element	**Existing Cross-Section (ft)**	**Dimensions After Optimization (ft)**			
		Curve (1)	Curve (3)	Curve (4)	Curve (5)
Inner carriageway shoulder	4.90	11.60	11.60	11.60	11.60
Inner carriageway lanes	11.50	9.00	9.00	9.00	9.00
Outer carriageway shoulder	4.90	0.00	0.00	0.00	0.00
Outer carriageway Lane	11.50	9.00	9.00	9.00	9.00
Median	6.60	14.80	14.80	14.80	14.80
Right of Way	62.40	62.40	62.40	62.40	62.40

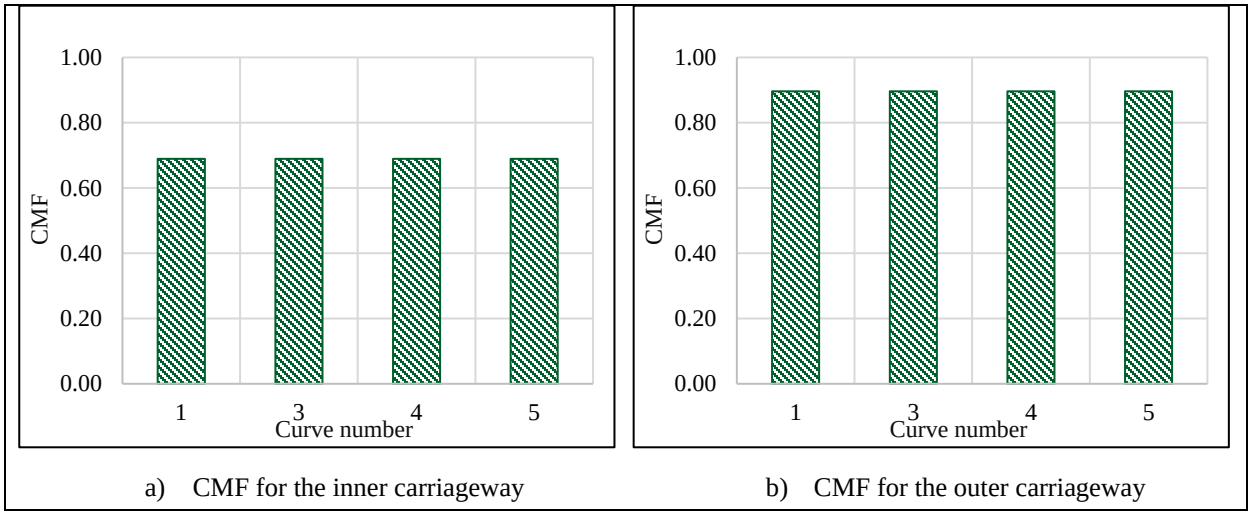

a) CMF for the inner carriageway

b) CMF for the outer carriageway

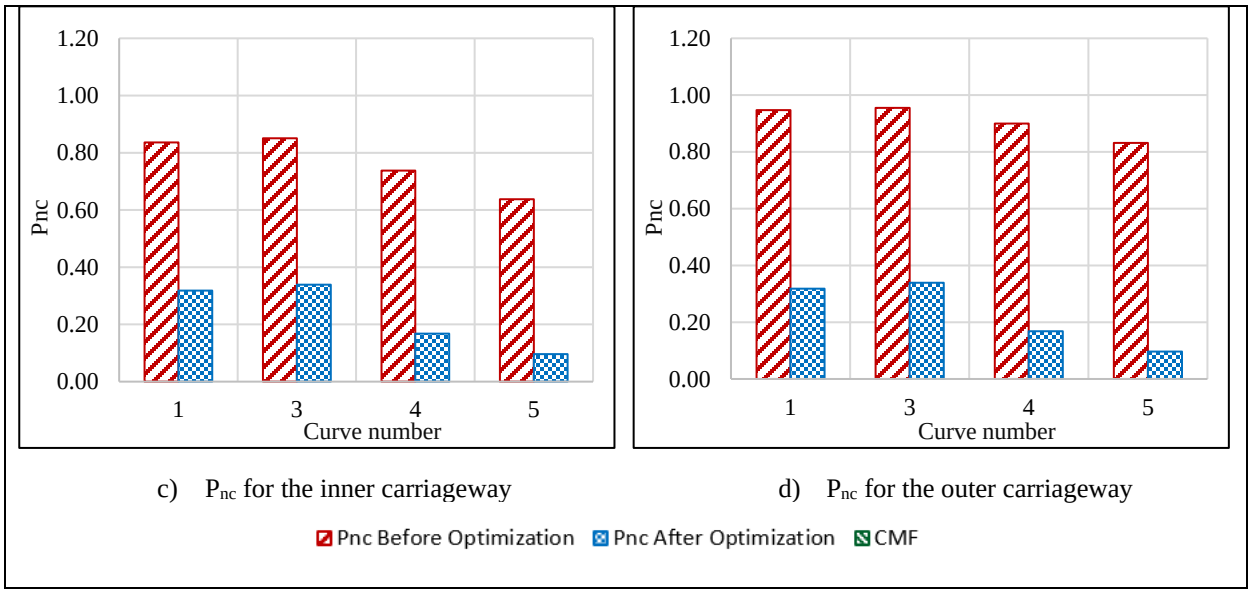

c) P_{nc} for the inner carriageway

d) P_{nc} for the outer carriageway

Figure 2.5: CMF and P_{nc} before and after optimization (Scenario III)

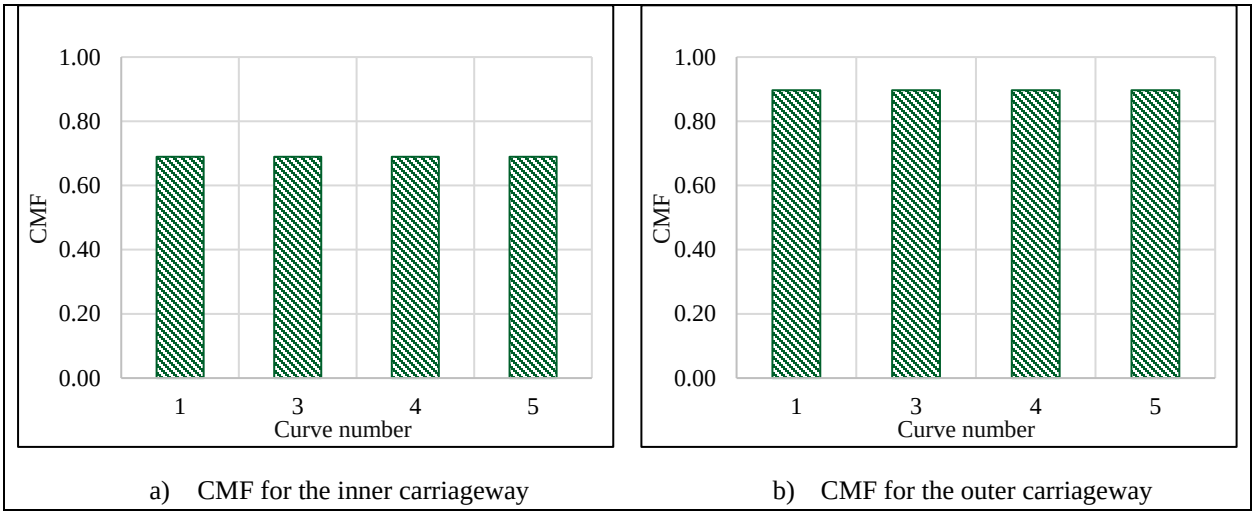

a) CMF for the inner carriageway

b) CMF for the outer carriageway

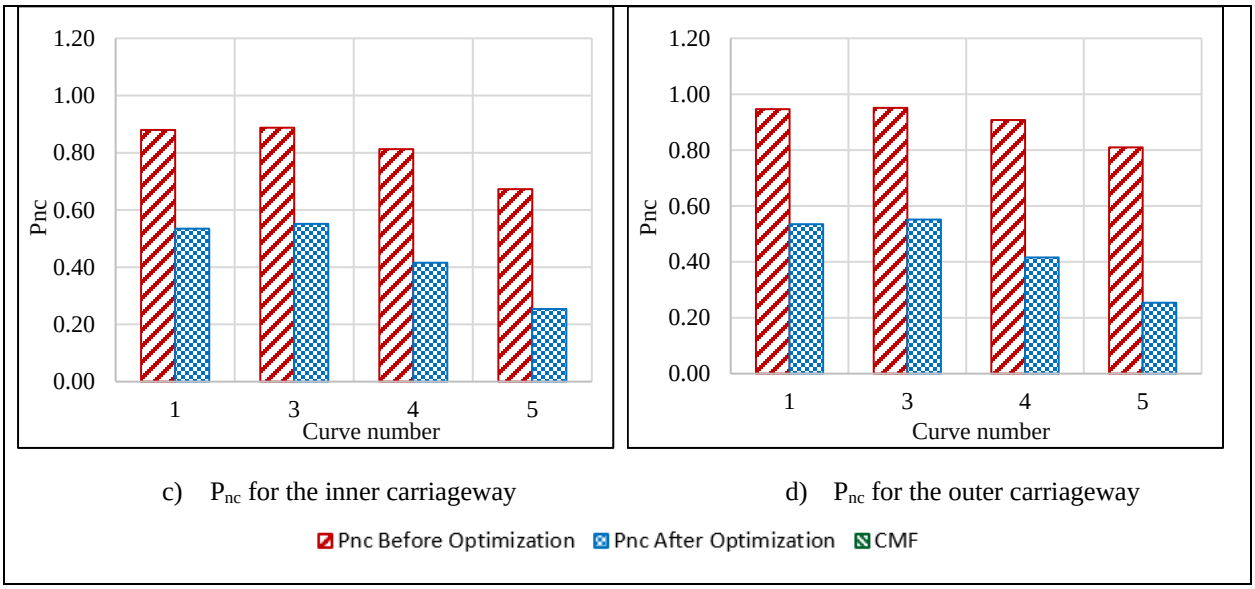

Figure 2.6: CMF and P_{nc} before and after optimization (Scenario IV)

Developing a Combined Safety Measure for CMF and P_{nc}

The results of the four scenarios (Scenario I through IV) showed that regardless of the prevailing conditions of each scenario (design versus operating speed or under-designed versus standard curve radii), the optimization yields similar results. The re-dimensioning is achieved by reducing the widths of all lanes to 9 ft, eliminating the shoulder of the outer carriageway, and use the spared width to increase the width of the inner carriageway shoulder and the median. By doing this, the available sight distance in both carriageways is maximized, the expected collision frequency is decreased by increasing the median width and reducing lane width. The negative impact of eliminating the outer carriageway shoulder on collision frequency is often compensated through the lane reduction and the median expansion. However, despite the similar cross-section configuration in all cases, the risk (P_{nc}) associated with each curve in each scenario varies significantly.

In order to enable a comprehensive understanding of the safety consequences of the cross-section optimization and facilitate conducting Cost-Benefit analysis, developing a combined measure that integrates the CMF and the P_{nc} in one unified safety measure would be of great significance. To that end, the relationship between the risk measure (P_{nc}) and collision, established by Ibrahim et al. (Ibrahim, et al., 2011), was used to convert the change in (P_{nc}) before and after optimization into a change in collision frequency (CMF). Ibrahim et al. (Ibrahim, et al., 2011) incorporated the P_{nc} in the collision prediction models of rural multi-lane highways as follows:

$$collisions\ (3years) = e^{-14.931} \times L \times v^{0.895} \times e^{1.461P_{nc}} \quad (16)$$

Where (L) is the length of the road segment and (V) is the total traffic volume. Assuming that all parameters remain constant except for the P_{nc}, the ratio between the expected collisions before and after changing the P_{nc} value can be calculated as follows:

$$CMF_{Pnc} = \frac{Collisions\ (After)}{Collisions\ (Before\ )} = \frac{e^{-14.931} \times L \times v^{0.895} \times e^{1.461Pnc(After)}}{e^{-14.931} \times L \times v^{0.895} \times e^{1.461Pnc(Before)}} = \frac{e^{1.461Pnc(After)}}{e^{1.461Pnc(Before)}} \quad (17)$$

Once the CMF corresponding to the change in the P_{nc} is determined, a $CMF_{combined}$ that integrates CMF of the inner and outer carriageways and the CMF_{Pnc} can be calculated according to Equation 18, as follows:

$$CMF_{combined} = CMF_{Total-I} \times CMF_{Total-O} \times CMF_{Pnc} \quad (18)$$

The $CMF_{combined}$ was developed for the five curves in the four scenarios addressed in the analysis, as shown in Figure 2.7. As shown in the figure, a significant reduction in collision frequency can be achieved through the optimization of the dimensions of different cross-section elements. The reduction is achieved by providing more lateral distance between vehicles and barriers, increasing the median and outer shoulder widths, and reducing lane widths. On average, a $CMF_{combined}$ of 0.35, 0.38, 0.26, and 0.33 was achieved in the four scenarios, respectively. This shows that the optimization of the cross-section elements can be an effective countermeasure that can reduce the collision frequency by more than 60% at tight curves with limited sight distance. Figure 2.7 clearly shows that the overall safety benefits resulted from the optimization are dependent on the speed treatment in the model (design speed versus operating speed). As such, it is recommended to consider accurate speed distributions that are calibrated for field conditions to undertake such an optimization problem. The results presented in Figure 2.7 are useful in assessing the safety benefits of the cross-section re-dimensioning in different scenarios, which is a cornerstone in assessing the economic viability of such a treatment and comparing between different design alternatives.

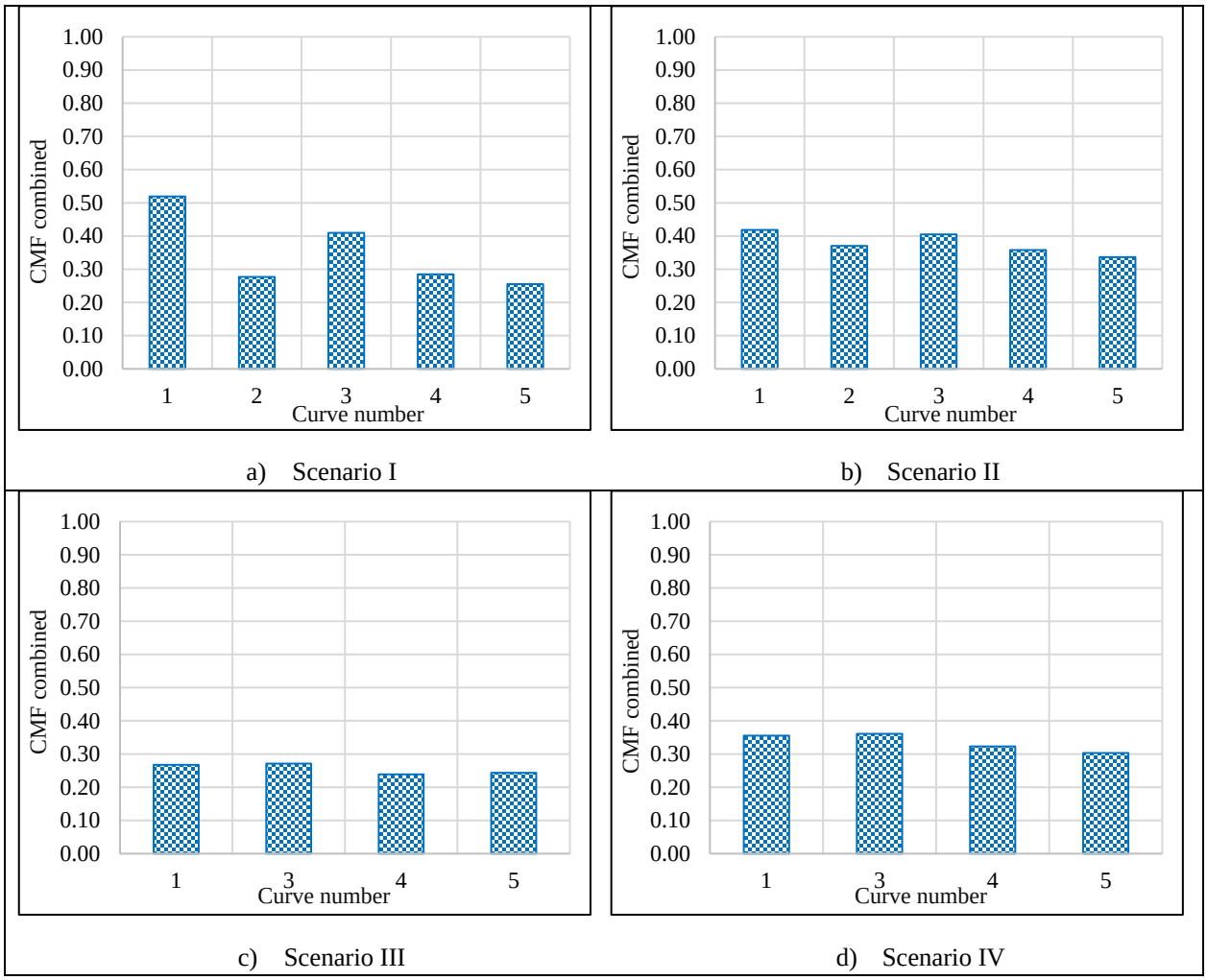

Figure 2.7: Combined Crash Modification Factor (CMF) for different optimization scenarios

Sensitivity Analysis

The sensitivity of the optimal dimensions of the cross-section elements and the $CMF_{combined}$ with respect to the mean value of the random input variables (i.e., PRT, acceleration rate, and operating speed) was assessed by means of a sensitivity analysis, as presented in Figure 2.8. In terms of the optimal dimensions of the different cross-section elements, the PRT was found to be the least sensitive parameter. Also, the optimal results were found to be not sensitive to changes in the deceleration rate. Increasing the mean value of the deceleration rate by up to 50% did not impact the optimization results at all. The change in the optimal section was only noted when the mean value of the deceleration rate dropped by more than 20%. The operating speed was found to be the most sensitive parameter on the optimal section results. Increasing the mean operating speed by more than 10% would change the optimal dimensions significantly. In terms of the $CMF_{combined}$, the change in the three parameters yields similar changes in the

resulted CMF, with the exception of large changes in operating speed. Changing both PRT and acceleration rate by up to 50% resulted in a maximum change of 20% for the $CMF_{combined}$. The results are very sensitive to small changes in the operating speed (±10%) before the model becomes more stable to changes in the operating speed. Based on the sensitivity analysis results, operating speed distribution seems to be critical for the accuracy of the results. Future studies should develop accurate operating speed distributions for the highways of interest to ensure the accuracy of the resulted cross-sections and the corresponding change in collision frequency.

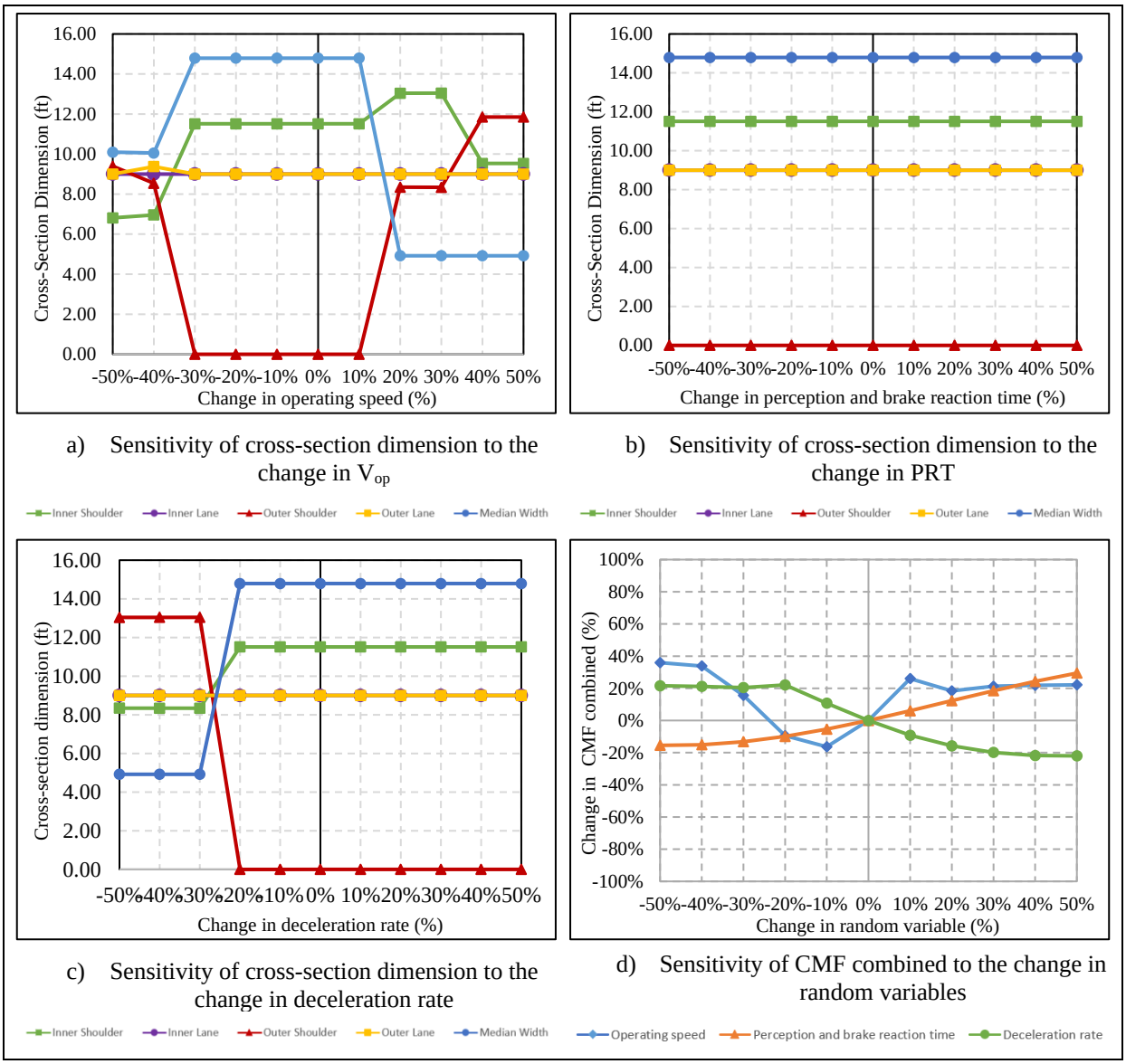

a) Sensitivity of cross-section dimension to the change in V_{op}

b) Sensitivity of cross-section dimension to the change in PRT

c) Sensitivity of cross-section dimension to the change in deceleration rate

d) Sensitivity of CMF combined to the change in random variables

Figure 2.8: Sensitivity analysis for random variables

Generalized Optimization Scenario

The four scenarios considered in the analysis did not consider changing the Right of Way (ROW) of the highway. It is understood that increasing the ROW would enable to provide adequate sight distance and reduce the risk (P_{nc}) to significantly lower levels. However, such a decision is also associated with a considerable increase in cost, especially in mountainous environments where the cost of the excavation and the supporting structures is usually huge. In order to aid the designers and planners with the economic analysis and selecting the optimal decision, a more generalized scenario was considered, in which the optimization was applied to determine the optimal cross-section elements of horizontal curves with different radii and different ROWs. Figure 2.9 shows the $CMF_{combined}$ of the resulted cross-sections (after optimization) for the first curve, considering different curve radii (160 – 260 m or 520-850 ft) and different ROWs (18 – 24 m or 60 – 78 ft). The results shown in the figure were developed considering the operating speed distribution, presented in Figure 2.1. The goal is to provide a powerful tool to assess the expected safety benefits corresponding to different decision alternatives so that the economic value of the reduction in the collision can be compared to the additional construction cost. As shown in Figure 2.9, the collision reduction resulting from the optimization ranges from 58% if the current radius and ROW are maintained to 81% with an increase of the ROW by 15.7 ft and increasing the curve radius to the standard AASHTO value.

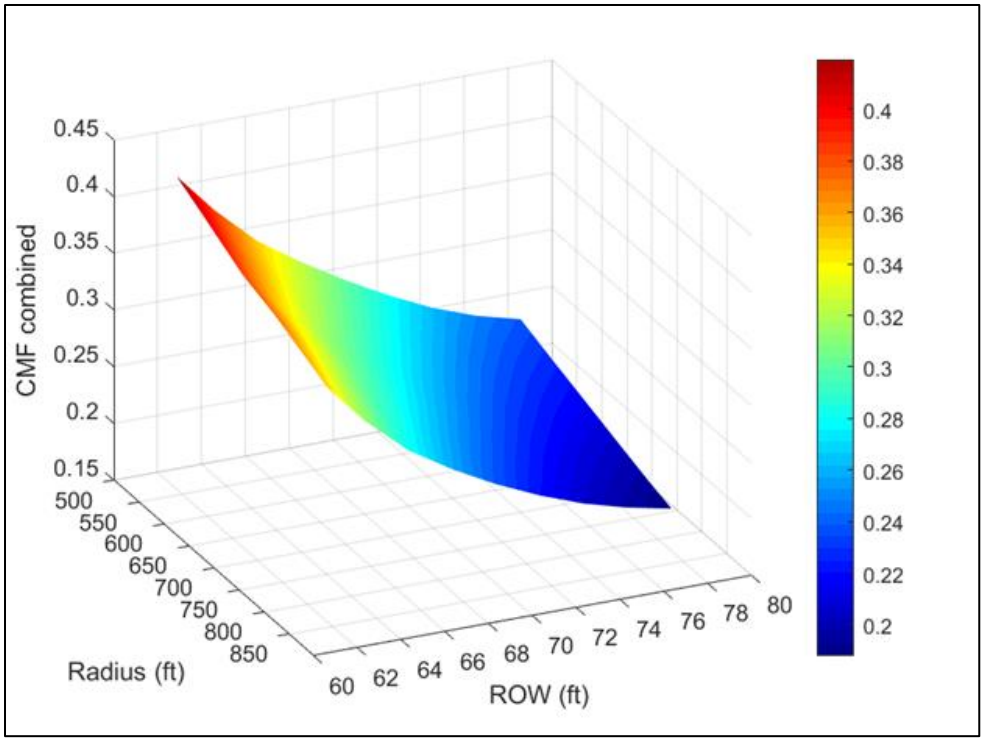

Figure 2.9: Combined CMF for different curve radii and ROWs

Conclusion and Future Work

This paper presented a framework for the optimization of the cross-section elements of horizontal curves with insufficient sight distance, along with assessing the safety benefits associated with the optimal cross-section. The study implemented a multi-objective optimization algorithm to select the optimal cross-sections of horizontal curves to minimize the risk associated with the limited sight distance (P_{nc}), minimize the expected collision frequency associated with the proposed cross-section, and ensure a balanced risk distribution between the inner and the outer carriageways. The concept was then applied on five restricted horizontal curves, located along the Sea-to-Sky Highway in British Columbia, which are satisfying neither the minimum radius nor the sight distance requirements recommended by AASHTO. The optimal sections and the corresponding reduction in collision frequency and improvement in P_{nc} were reported for four analysis scenarios. The four scenarios consider both design and operating speed at the existing curve radii (Scenarios I and II) and the design and operating speed at the standard curve radii, recommended by AASHTO (Scenarios III and IV). Finally, a more generalized scenario was considered, in which the optimization was applied to determine the optimal cross-section elements of horizontal curves with different radii and different ROWs. The study also introduced a unified safety measure ($CMF_{combined}$) that integrates the change in collision frequency and the P_{nc} in

one measure that is capable of providing a better assessment of the safety benefits of the proposed methodology.

The results showed a considerable reduction in the inherent risk as well as the collision frequency as a result of the re-dimensioning of the cross-section elements in all scenarios. The combined reduction in collision frequency resulting from optimization ranged between 48% to 74% in the first scenario (considering the design speed), and 58% to 66% in the second scenario (considering the operating speed). Increasing the curve radii to the standard values, recommended by AASHTO, help to achieve a further reduction in the collision that ranged between 1% to 25% in the third scenario (considering the design speed), and 3% to 6% in the fourth scenario (considering the operating speed). When a more generalized case was considered, the collision reduction resulting from the optimization was shown to vary between 58% if the current radius and ROW are maintained to 81% with an increase of the ROW by 15.7 ft and increasing the curve radius to the standard AASHTO value. The results highlighted the significant impact of the speed treatment (design speed and operating speed) on the results, so it was recommended to rely on reliable operating speed models when conducting such analyses.

Nevertheless, the current study is subject to some limitations that need to be addressed in future studies, First, the operating speed models and the methodology used to convert the risk (P_{nc}) into collision frequency are both based on previous studies that were not developed particularly for the five curves considered in the study. Although it is expected that the impact on the results would be minimal, future studies should consider developing their own operating speed distributions and collision prediction models to conduct the analyses. Also, the weighted-sum multi-objective optimization technique is subject to shortcomings such as missing the non-convex Pareto optimal points, and the difficulties of normalizing the objectives for more than two objective functions. Future studies should investigate the application of other multi-objective organization methods and examine whether the results will be impacted by the optimization method implemented. Moreover, future studies should investigate the conversion of the P_{nc} to a direct safety measure (CMF_{pnc}) in detail to develop a more reliable unified safety measure ($CMF_{combined}$). This will require collecting collision data at the studied highway and develop collision prediction models that include P_{nc} as an explanatory variable. Once achieved, the optimization problem can be converted to a single objective optimization that aims at minimizing the unified safety measure ($CMF_{combined}$) to overcome the multi-objective optimization drawbacks. Also, the optimization problem can be expanded by adding the construction cost to the objective function. The construction cost is directly related to the curve radius and the ROW, which will be considered

as additional decision variables in this case. Such a decision will enable the selection of the optimal dimensions of the cross-section elements that maximize the safety benefits and minimize the construction cost at the same time. In addition, the potential correlation between different design parameters (i.e., reaction time, driver deceleration, and operating speed) was not considered. Future studies should investigate the impact of such a correlation on the results. The current study also considers one mode of non-compliance on the horizontal curves (i.e., the limited sight distance). Other modes of non-compliance were not considered (e.g., skidding and rollover). Future studies should consider implementing a system reliability approach that considers all potential modes of non-compliance to conduct the analyses. Finally, the current study neglected the potential correlation between the safety impacts of the limited sight distance (CMF_{pnc}) and the collision reduction associated with the different cross-section elements.

CHAPTER 3: CONCLUSIONS AND PRACTICE IMPLICATIONS

Conclusion

The current study presented a framework for optimizing the cross-section elements of horizontal curves with limited sight distance. The study utilized a multi-objective optimization technique to select the optimum cross-section elements combination to minimize the risk associated with the inadequate sight distance, minimize the expected collision frequency, and balance the risk between the two directions. The optimization was applied on five tight horizontal curves in the southern section of the Sea-to-Sky Highway in British Colombia. The five curves of interest failed to satisfy neither the minimum curve radius nor the sight distance requirements suggested by AASHTO. Four analysis scenarios were considered, by considering both design and operating speed at the exiting curve radii (Scenario I and II) and both design and operating speed at the standard curve radii recommended by AASHTO (Scenario III and IV). Also, a unified safety measure was introduced by integrating the P_{nc} and the change in collision frequency (CMF) in a measure named $CMF_{combined}$. This unified safety measure helped in evaluating the benefits of the optimization and was used in developing a generalized model where the $CMF_{combined}$ was calculated for optimizing the cross-section for different curve radii and ROWs.

It was observed that the risk associated with the limited sight distance and the collision frequency reduced significantly in all scenarios as a result of cross-section optimization. In scenario I, the combined reduction in collisions due to the cross-section re-dimensioning ranged between 48% to 74%, while in scenario II, the combined reduction in collisions ranged between 58% to 66%. The additional reduction in the collisions due to increasing the curve radius to the standard values in scenario III was increased by 1% to 25% than scenario I, while it was increased in scenario IV by 3% to 6% than scenario II. The generalized model developed for the first curve showed a collision reduction varied between 58% when the curve radius and the ROW are maintained, while a significant reduction in collisions by 81% when the curve radius increased to the standard value and the ROW increased by 15.7 ft. The speed treatment showed a significant impact on the results and highlights the importance of utilizing a reliable operating speed distribution in future analysis. The following section provides an example of economic analysis, in which the results of the generalized model are used to estimate the savings resulted from collision reduction. The additional construction cost corresponding to different values of curve radius and ROW was also estimated so that the B/C of different design alternatives can be calculated.

Practice Implication

It is widely acclaimed that designing roads to be ultimately safe in restricted environments would be extremely costly. As such, the trade-off between cost and safety is the most challenging dilemma faced by designers in such environments. The case addressed in this study (i.e., the design of horizontal curves in mountainous terrains) is a clear example of such a dilemma. As discussed earlier, meeting the design standards for horizontal curves in mountainous terrains is considerably challenging and is often associated with a significant increase in the construction cost (i.e., rock-cut cost, paving cost, roadside barrier and signing relocation, site grading cost). Since there is no direct link between design standards and objective measures of safety, designers are not able to estimate the expected collision reduction (CR) that will result from the additional construction cost, and consequently, conducting a cost-benefit analysis to justify the additional construction cost is not possible. Luckily, the generalized model developed in this study (Figure 2.9) provides a powerful tool to estimate the expected reduction in collisions corresponding to different Right of Way and curve radius values. This enables to conduct a cost-benefit analysis, in which the designer can assess the benefits corresponding to the additional construction cost through a B/C ratio and/or determine the point at which the construction cost breaks even with the expected savings from collision reduction.

The following section provides a sample cost-benefit analysis for the first curve. The existing curve is very tight (radius = 160 m, way smaller than the 252 m standard radius required by AASHTO). The analysis will explore the economic benefit of increasing the curve radius from 160 m to 252 m and estimate the optimal curve radius to target based on the observed collision frequency on the curve so that the additional construction cost of increasing the curve radius matches the savings resulting from reducing collision frequency. Such analysis will aid designers to find a balance between safety and construction cost and support them to make informative decisions that consider geometric design considerations, safety, and budget.

Cost-Benefit Analysis

The benefit to cost ratio (B/C) was used to evaluate the economic benefit of increasing the radius of the first curve. The optimized cross-section of the existing curve (R = 160 m and $CMF_{combined}$ = 0.419) was used as a base case for comparison. Curve radii between the existing radius (160 m) to the standard recommended by AASHTO (252 m), with an increment of 20 meters, were considered in the analysis. For each curve radius, the expected crash modification factors corresponding to the curve radius (after optimizing the cross-section elements) were estimated from Figure

2.9. The additional construction cost required to increase the curve radius from 160 m to each of the curve radii considered in the analysis were estimated according to the procedures presented in the following section. Finally, a critical number of collisions corresponding to each curve radius was determined. This critical collision frequency was determined so that the additional construction cost equals the savings resulted from collision reduction at each curve radius (i.e., B/C = 1). A critical collision frequency curve was developed for different curve radii. Designers can use this curve to determine the most economic curve radius to target, based on the observed (or the expected) number of collisions on the curve. The details of the analysis are presented as follows:

Additional construction cost

The first curve is located in the southern end of the Sea-To-Sky Highway (exactly, 600 m from the beginning of the highway) Figure 3.1 shows a satellite image of the curve. As shown in the figure, the curve is a right-hand curve that is restricted by the mountainous terrain from the east side, making the radius increase a very challenging and costly task.

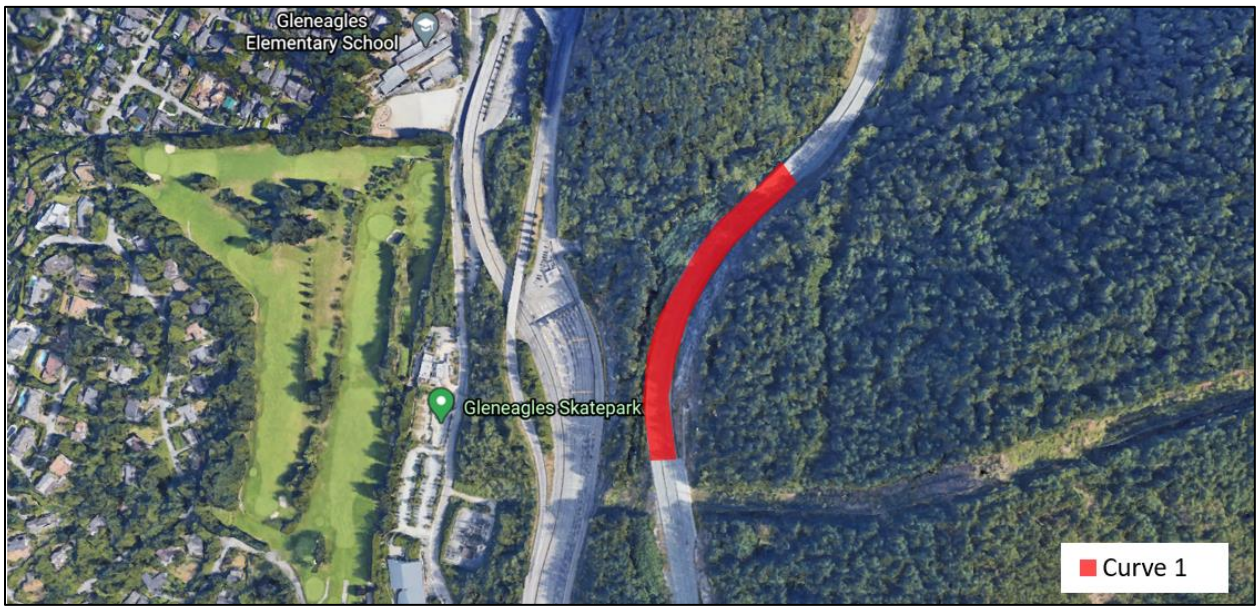

Figure 3.1: Curve 1 plan and cross-section.

For the curve radius to be increased, the rocks to the east of the curve must be cut to provide a space for the wider curve. Based on the topographic maps of the area, it is estimated that the average height of the rocks on the east side of the curve in this area is 50 m. As for the additional area needed to increase the curve radius, Figure 3.2 shows

the additional cut areas for different radii starting from the existing curve radius (160 m) to the standard radius (252 m).

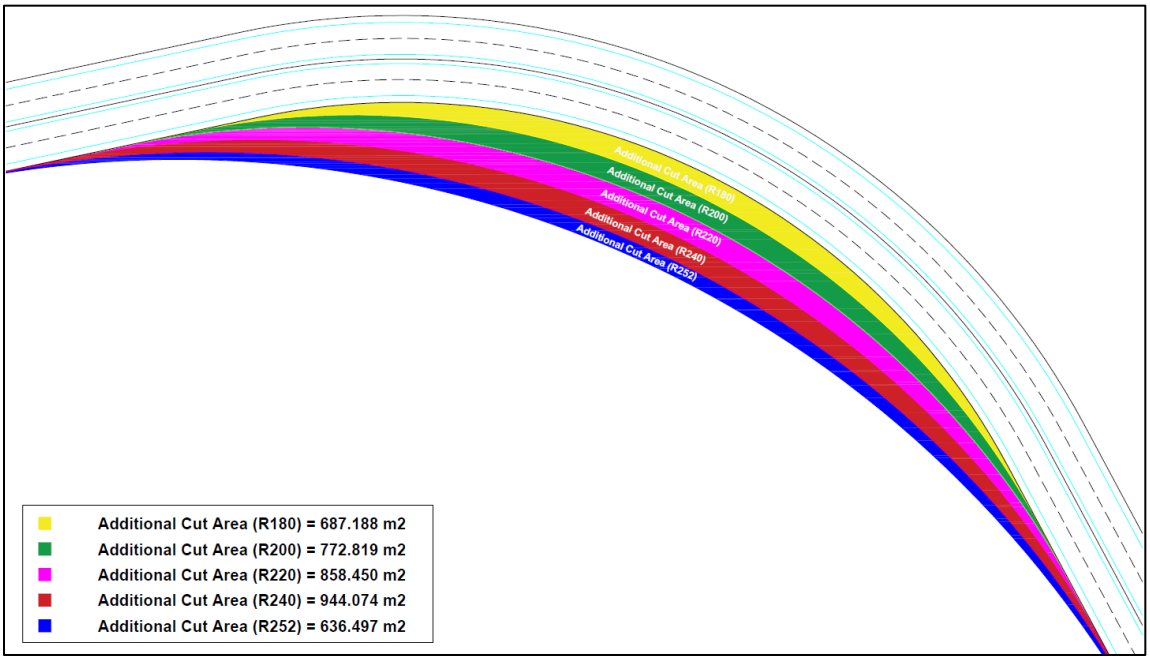

Figure 3.2: Curve 1 additional cut areas.

In addition to the rock-cut cost, it is essential to estimate the cost of additional pavement corresponding to different curve radii. An estimate about the pavement thickness was obtained from the pavement structure design guideline, published by the BC Ministry of Transportation and Infrastructure (Daryl, et al., 2015). The unit cost of the required earthwork and the different pavement layers were determined based on a cost estimate system published by the British Columbia Ministry of Transportation and Infrastructure (Highway planning Cost Estimating System (HCES)), as presented in Table 3.1. The earthwork and pavement material costs corresponding to the different course radii are then estimated according to Equations 19-21. It should be noted that the total cost resulted from Equations 19-21 was increased by 15% to account for other costs that are not considered in the analysis (such as the cost of the relocation of signs and street lighting, the cost of moving the roadside barriers, the cost of the pavement marking, among other costs). Future studies should conduct a more comprehensive Cost-Benefit analysis that accounts for risk assessment, road construction, site preparation, utilities, and operational costs.

$$Cut\ cost = additional\ cut\ area \times average\ cut\ height \times unit\ price \quad (19)$$

$$Coat/Asphalt\ cost = additional\ cut\ area \times\ unit\ price \quad (20)$$

$$Base/Subbase\ cost = additional\ cut\ area \times Layer\ thickness \times\ unit\ price \quad (21)$$

Table 3.1: Earthwork and paving unit costs

Item	Units	Unit Rate
Rock Excavation	cubic meter	$ 20.00
Asphalt Pavement	squared meter	$ 32.3
Prime Coat	squared meter	$ 0.50
Tack Coat	squared meter	$ 0.50
Crushed Base Coarse (CBC)	cubic meter	$ 22.00
Subbase (SGSB)	cubic meter	$ 15.00

Collision Cost Saving

The cost of the expected collision reduction corresponding to the different curve radii was calculated to evaluate the economic benefit of increasing the curve radius. The cost of collisions was obtained from a 2018 report, published by the British Columbia Ministry of Transportation and Infrastructure (BC Ministry of Transportation and Infrastructure, 2018), as shown in Table 3.2. It should be noted that the collision costs reported in (BC Ministry of Transportation and Infrastructure, 2018) were reported in 2018 Canadian dollars. The costs were adjusted for inflation, using an average inflation rate of 1.2% between 2018 and 2020.

Table 3.2: Cost of collisions

Collision Type	Adjusted Cost of Collision (2020 CAD)
Fatal Collision	$ 8,381,851
Serious Collision	$ 313,673
PDO Collision	$ 14,011

The expected reduction in collisions frequency per year resulting from the increase in the curve radius was obtained from the generalized model shown in Figure 2.9, and the cost of the reduced collisions was calculated according to Equations 22-24.

$$CR = CMF_{combined(160)} - CMF_{combined(Rnew)} \quad (22)$$

$$Expected\ reduction\ in\ collision\ = CR \times observed\ collision \quad (23)$$

$$Annual\ Collisions\ saving\ cost\ = Expected\ reduction\ in\ collision \times Cost\ of\ collision \quad (24)$$

The expected annual reduction in collision saving was converted to present worth value (PW), according to Equations 25-26 to enable the calculation of the B/C ratio, shown in Equation 27. The service life of the highway (n) was assumed to be 15 years. A discount rate of 0.25% was used, based on the Bank of Canada (Bankofcanada.ca).

$$SPWF\ = \frac{(1+i)^n-1}{i\times(1+i)^n} \quad (25)$$

$$PW\ = SPWF \times Collisions\ saving\ cost \quad (26)$$

$$B/C\ = \frac{PW}{Total\ construction\ cost} \quad (27)$$

Where:

SPWF	Series Present Worth Factor
i	The discount rate
n	Number of years

Critical Collision Frequency Curve

Since the collision record on the curve is not available, the cost-benefit analysis was conducted for a range of annual collision frequency. First, the cost-benefit analysis was conducted for fatal collision frequencies that ranged between 0 to 1 collision per year, with an increment of 0.1. Second, the analysis was conducted for serious collision frequencies that ranged between 0 to 20 collision/year, with an increment of 1. To help the designer selecting the optimum curve radius, a critical curve was developed for both fatal collisions and serious collisions, as shown in Figure 3.3. The critical curves show the optimal curve radius corresponding to an observed collision frequency so that the increase in the construction cost matches the savings in collision reduction (i.e., B/C=1). For example, if the curve experienced 12 serious collisions per year, increasing the curve radius to 215 m would be justified (B/C = 1). Similarly, if the curve witnessed 0.5 fatal collisions per year (1 fatal collision every two years), the curve radius should be increased to 230 m.

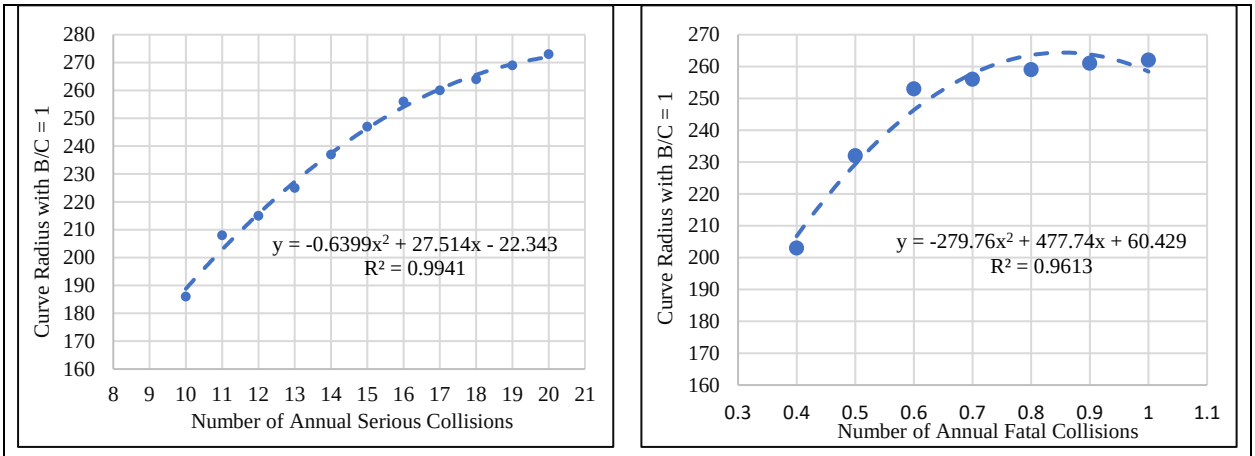

a) Critical collision frequency curve (serious collision) b) Critical collision frequency curve (Fatal collision)

Figure 3.3: Critical collision frequency curve.

It was observed that increasing the curve radius will not be economically beneficial if the number of serious collisions occurs at the curve is below 10 serious collisions per year. On the other side, increasing the curve radius will not be economically beneficial if the number of serious collisions occurs at the curve is below 0.4 fatal collisions per year (2 fatal collisions in 5 years).

It is recommended for future studies to consider other costs that were not considered in the current analysis (such as pavement marking, rumble strips, site preparation, the relocation of barriers, signs, and street lighting) to develop a more accurate estimation of the B/C ratio. Moreover, future studies should conduct the cost-benefit analysis for different combinations of serious and fatal collisions or rely on the actual collision frequency that is recorded at the curve of interest.

REFERENCES

AASHTO Part D Highway safety manual [Book]. - Washington, DC : AASHTO, 2010.

Abdel-Aty M. A. [et al.] Validation and application of highway safety manual (part D) in Florida Florida. [Report] / Dept. of Transportation. ; Florida. Dept. of Transportation. - 2014.

Alfredo H. S. A. and Wilson H. Probability Concepts in Engineering Planning and Design: Vol. I-Basic Principles. [Journal] // The Statistician. - 1979. - 3 : Vol. 28.

Ang A.H-S. and Tang W.H. Probability Concepts in Engineering Planning and Design [Book Section] // Vol. 1, Basic principles (No. BOOK). - 1975.

Ang A.H-S. and Tang W.H. Probability COncepts in Engineering Planning and Design [Book Section] // Vol. 1, Basic principles (No. Book). - 1975.

BC Ministry of Transportation and Infrastructure Default Values for Benefit Cost Analysis In British Columbia 2018 [Report]. - 2018.

Branch BC Ministry of Transportation and Infrastructure Planning and Programming Default Values for Benefit Cost Analysis In British Columbia 2018 [Report]. - [s.l.] : BC Ministry of Transportation and Infrastructure Planning and Programming Branch, 2018.

Daryl F. and Sarah G. PAVEMENT STRUCTURE DESIGN GUIDELINES Technical Circular T-01/15 [Report]. - [s.l.] : British Columbia Ministry of Transportation and Infrastructure, 2015.

Easa S. M. and Cheng J. Reliability analysis of minimum pedestrian green interval for traffic signals [Journal] // Journal of transportation engineering. - 2013. - 7 : Vol. 139. - pp. 651-659.

Eiksund S. A geographical perspective on driving attitudes and behaviour among young adults in urban and rural Norway [Journal] // Safety Science. - [s.l.] : Elsevier, 2009. - 4 : Vol. 47. - pp. 529-536.

Ellingwood B. Development of a probability based load criterion for American National Standard A58: Building code requirements for minimum design loads in buildings and other structures. [Book Section] // Vol. 13. US Department of Commerce, National Bureau of Standards. - 1980.

Essa M., Sayed T. and Hussein M. Multi-mode reliability-based design of horizontal curves [Journal] // Accident Analysis & Prevention. - 2016. - Vol. 93. - pp. 124-134.

Faghri A. and D. Michael J. Reliability and ris assessment in the prediction of hazards at rail-highway grade crossings [Journal] // Transportation Research Record. - 1988. - Vol. 1160. - pp. 45-51.

Faghri A. and D. Michael J. Reliability and risk assessment in the prediction of hazards at rail-highway grade crossings [Journal] // Transportation Research Record. - 1988. - Vol. 1160 . - pp. 45-51.

Fambro D., Fitzpatrick K. and Koppa. R. NCHRP report 400: determination of stopping sight distances. national cooperative highway research program [Journal] // Transportation Research Board, National Research Council. Washington, DC: National Academy Press. - 1997.

Gross F. and Donnell E. Case–control and cross-sectional methods for estimating crash modification factors: Comparisons from roadway lighting and lane and shoulder width safety effect studies [Journal] // Journal of Safety Research. - 2011. - 2 : Vol. 42. - pp. 117-129.

Gross F. and Jovanis. P. Estimation of the safety effectiveness of lane and shoulder width: Case-control approach [Journal] // Journal of transportation engineering . - 2007. - 6 : Vol. 133. - pp. 362-369.

Gross F. Case–control analysis in highway safety: Accounting for sites with multiple crashes [Journal] // Accident Analysis & Prevention . - 2013. - Vol. 61. - pp. 87-96.

Guo H. [et al.] Reliability analysis of pedestrian safety crossing in urban traffic environment [Journal] // Safety Science. - 2012. - 4 : Vol. 50. - pp. 968-973.

Harkey D. L. Accident modification factors for traffic engineering and ITS improvements [Report]. - [s.l.] : (Vol. 617). Transportation Research Board., 2008.

Harwood D. W. [et al.] Systemwide impact of safety and traffic operations design decisions for 3R projects [Report] / TRB. - Washington, D.C. : NCHRP Report 486, 2003.

Hauer E. Lane width and Safety [Report]. - Toronto, Ontario : Draft document. Review of Literature for the Interactive Highway Safety Design Model, 2000.

Hauer E. Safety in geometric design standards. [Report]. - Toronto : University of Toronto, Department of Civil Engineering, 1999.

Highway planning Cost Estimating System (HCES) British Columbia Ministry of Transportation [Online] // https://www2.gov.bc.ca/gov/content/governments/organizational-structure/ministries-organizations/ministries/transportation-and-infrastructure.

Hussain A. and Easa S. M. Reliability analysis of left-turn sight distance at signalized intersections. [Journal] // Journal of transportation engineering. - 2016. - 3 : Vol. 142. - p. 04015048.

Hussein M. [et al.] Calibrating road design guides using risk-based reliability analysis. [Journal] // Journal of Transportation Engineering. - 2014. - 9 : Vol. 140. - p. 04014041.

Ibrahim S. E. B. and Sayed T. Developing safety performance functions incorporating reliability-based risk measures. [Journal] // Accident Analysis & Prevention. - 2011. - 6 : Vol. 43. - pp. 2153-2159..

Ibrahim S. E., Sayed T. and Ismail K. Methodology for safety optimization of highway cross-sections for horizontal curves with restricted sight distance. [Journal] // Accident Analysis & Prevention. - 2012. - Vol. 49. - pp. 476-485..

Ismail K. and Sayed T. Risk-based framework for accommodating uncertainty in highway geometric design [Journal] // Canadian Journal of Civil Engineering. - 2009. - 5 : Vol. 36. - pp. 743-753.

Ismail K. and Sayed T. Risk-based highway design: Case studies from British Columbia, Canada. [Journal] // Transportation Research Record: Journal of the Transportation Research Board. - 2010. - 1 : Vol. 2195. - pp. 3-13.

Ismail K. and Sayed T. Risk-optimal highway design: Methodology and case studies [Journal] // Safety science, . - 2012. - 7 : Vol. 50. - pp. 1513-1521.

Jacobs G., Aeron-Thomas A. and Astrop A. Estimating Global Road Fatalities [Report]. - Crowthorne, United Kingdom : Transport Research Laboratory, 2000.

Jones A.p. [et al.] Geographical variations in mortality and morbidity from road traffic accidents in England and Wales [Journal]. - [s.l.] : Health & Place, 2008. - 3 : Vol. 14. - pp. 519-535.

Jovanovic´ D., Backalic´ T. and Bašic S. The application of reliability models in traffic accident frequency analysis [Journal] // Safety Science. - 2011. - 8-9 : Vol. 49. - pp. 1246-1251.

Lee C. [et al.] Development of crash modification factors for changing lane width on roadway segments using generalized nonlinear models [Journal] // Accident Analysis & Prevention . - [s.l.] : Elsevier, 2015. - Vol. 76. - pp. 83-91.

Lerner N. Age and driver perception-reaction time for sight distance design requirements. [Journal] // Compendium of Technical Papers. Institute of Transportation Engineers 65th Annual Meeting. Institute of Transportation Engineers (ITE). - 1995.

Lord D. [et al.] Methodology to predict the safety performance of rural multilane highways [Report]. - [s.l.] : (No. NCHRP Project 17-29)., 2008.

Mahsuli M. and Haukaas T. Computer program for multimodel reliability and optimization analysis. [Journal] // Journal of Computing in Civil Engineering. - 2013. - 1 : Vol. 27. - pp. 87-98.

Pratt M. P. [et al.] Evaluating the need for surface treatments to reduce crash frequency on horizontal curves [Report]. - [s.l.] : Texas. Dept. of Transportation. Research and Technology Implementation Office., 2013.

Qin X., Ivan J. N. and Ravishanker N. Selecting exposure measures in crash rate prediction for two-lane highway segments [Journal] // Accident Analysis & Prevention . - 2004. - 2 : Vol. 36. - pp. 183-191.

Richl L. and Sayed T. Evaluating the safety risk of narrow medians using reliability analysis [Journal] // Journal of Transportation Engineering . - 2006. - 5 : Vol. 132. - pp. 366-375.

Sarhan M. and Hassan Y. Three-dimensional, probabilistic highway design: sight distance application. [Journal] // Transportation Research Record: Journal of the Transportation Research Board. - 2008. - 1 : Vol. 2060. - pp. 10-18.

Stamatiadis N. and Council. National Research Impact of shoulder width and median width on safety [Report]. - [s.l.] : (Vol. 633). National Academies Press., 2009.

Transportation British Columbia Ministry of Ministry of Transportation and Infrastructure [Online] // https://www2.gov.bc.ca/gov/content/governments/organizational-structure/ministries-organizations/ministries/transportation-and-infrastructure.

Wang J. [et al.] A novel train control approach to avoid rear-end collision based on geese [Journal] // Safety Science. - 2017. - Vol. 91. - pp. 373-380.

Wood S., J. and Donnell T., E. Stopping sight distance and horizontal sight line offsets at horizontal curves [Journal] // Journal of the Transportation Research Board . - 2014. - 1 : Vol. 2436. - pp. 43-50.

World Health Organization Global status report on road safety 2018: Summary [Report] / World Health Organization. - Geneva, Switzerland : No. WHO/NMH/NVI/18.20. World Health Organization., 2018.

Yue L. [et al.] In-depth approach for identifying crash causation patterns and its implications for pedestrian crash prevention [Journal] // Journal of Safety Research. - 2020. - Vol. 73. - pp. 119-132.

APPENDIX A_1

Figures 5.1 to 5.4 present the generalized model for curves 2, 3, 4 and 5. The figures provide the $CMF_{combined}$ corresponding to different ROWs and curve radii.

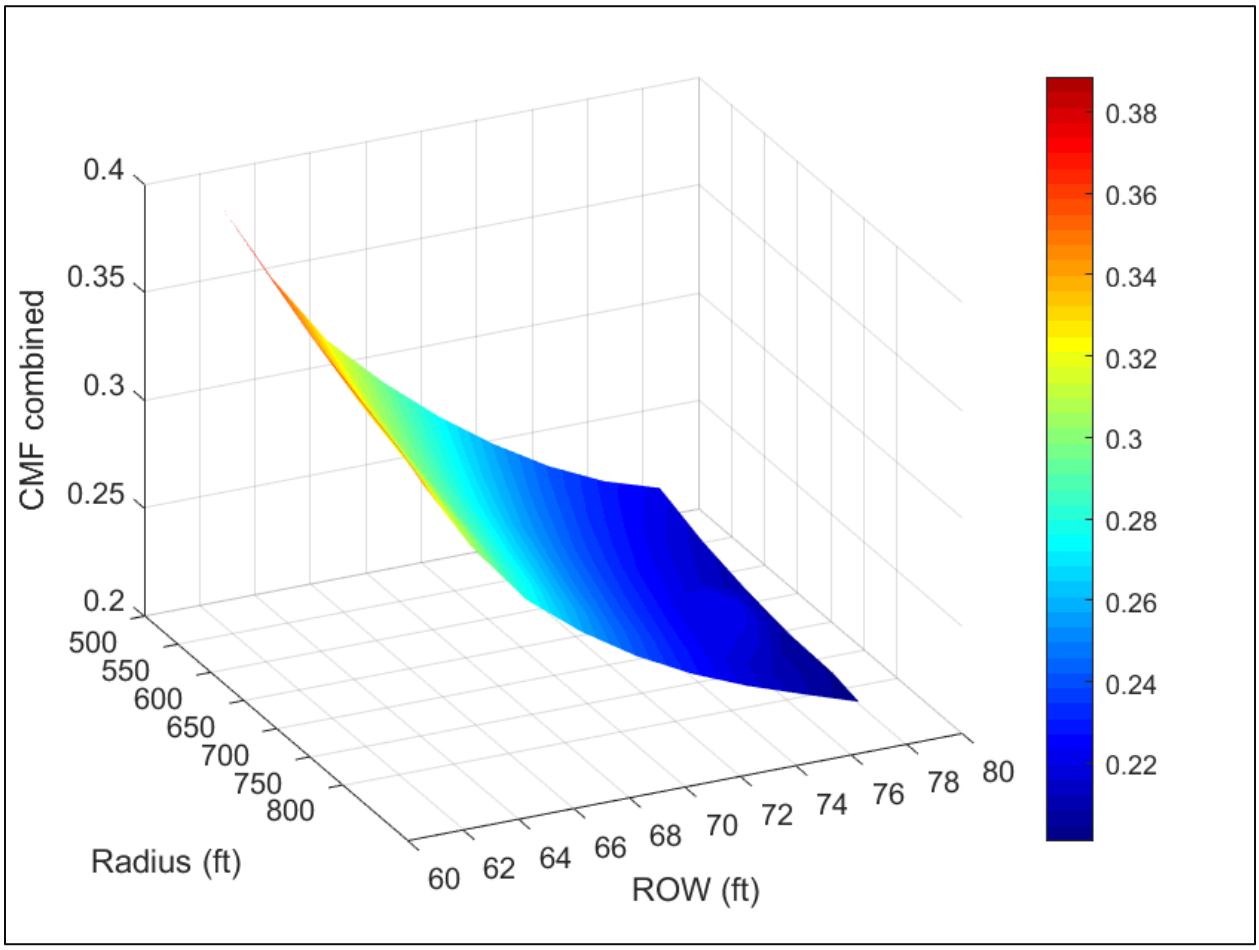

Figure 5.1: Combined CMF for different curve radii and ROWs (Curve 2)

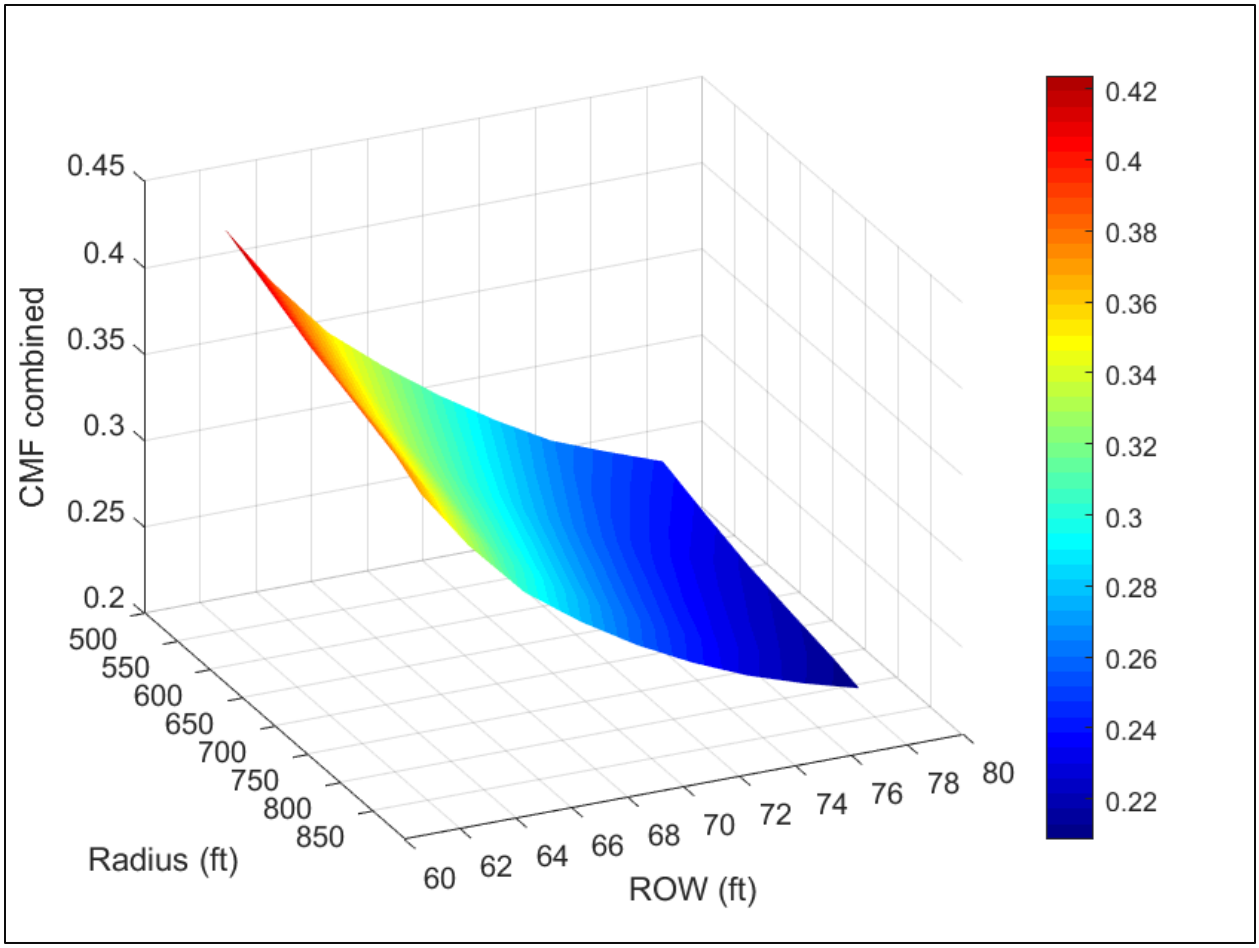

Figure 5.2: Combined CMF for different curve radii and ROWs (Curve 3)

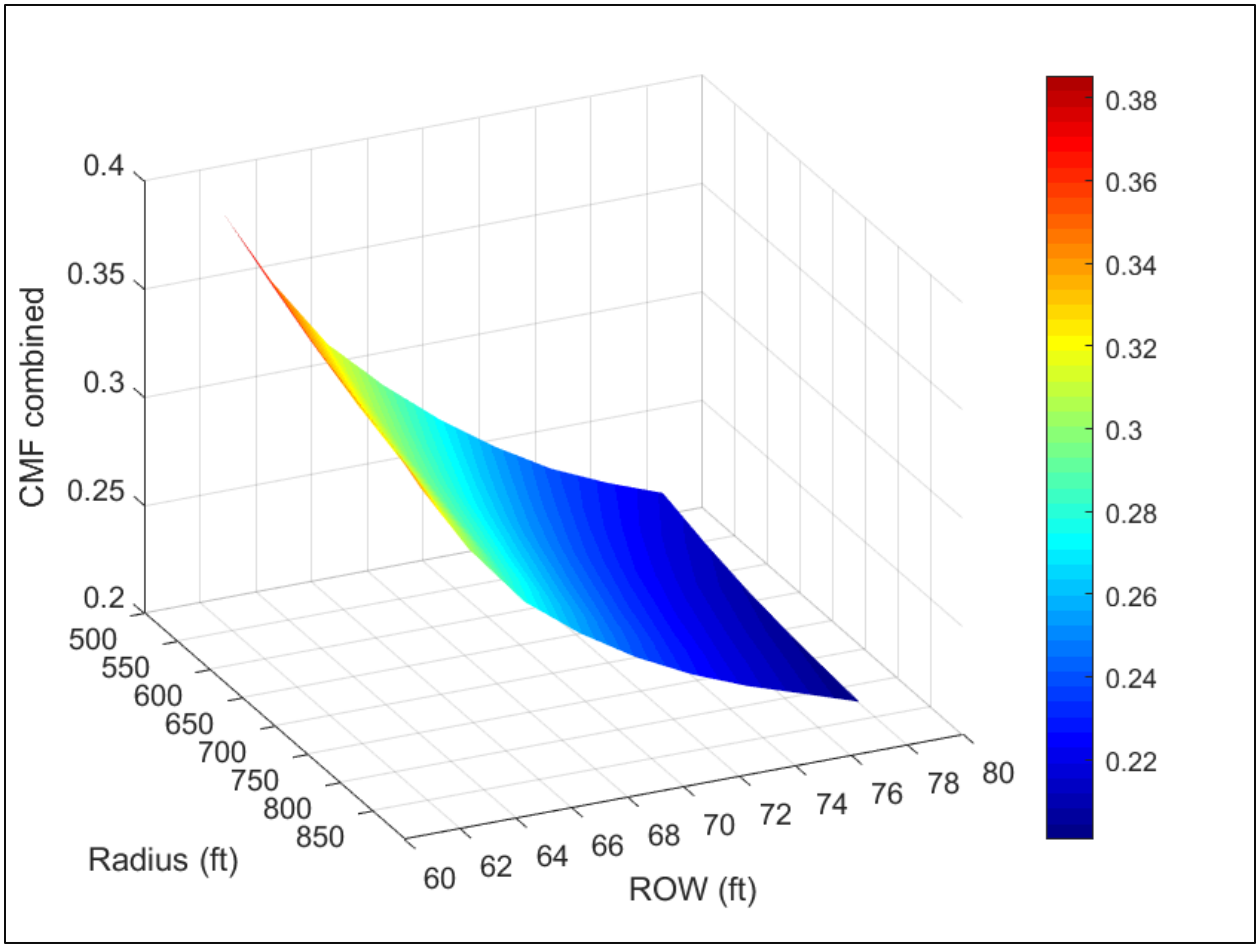

Figure 5.3: Combined CMF for different curve radii and ROWs (Curve 4)

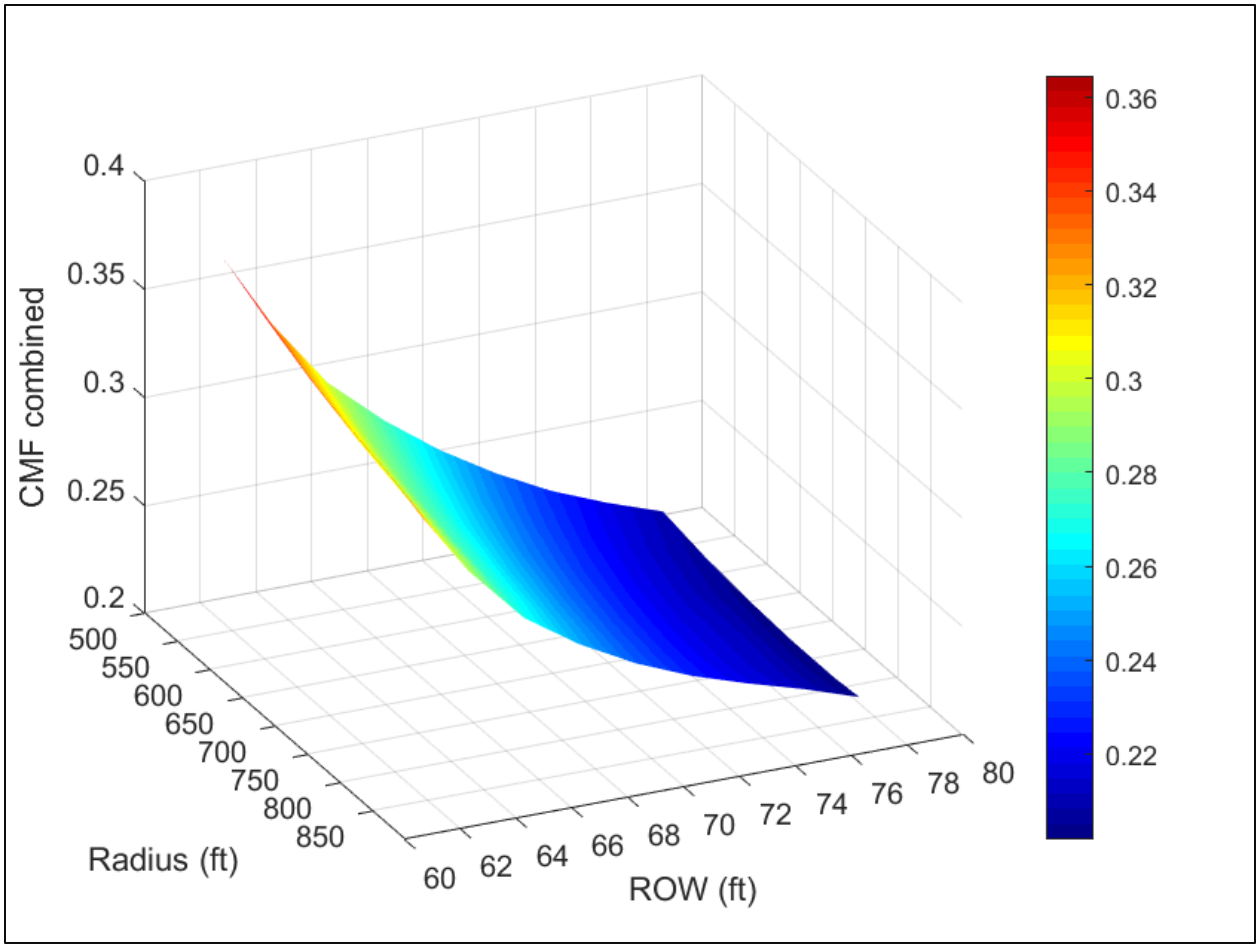

Figure 5.4: Combined CMF for different curve radii and ROWs (Curve 5)

APPENDIX A_2

Figures 5.5 to 5.8 present the sensitivity analysis for curves 2, 3, 4 and 5. The figures show the sensitivity of the cross-section elements and the $CMF_{combined}$ to the change in the random variables (V_{op}, PRT, and deceleration rate)

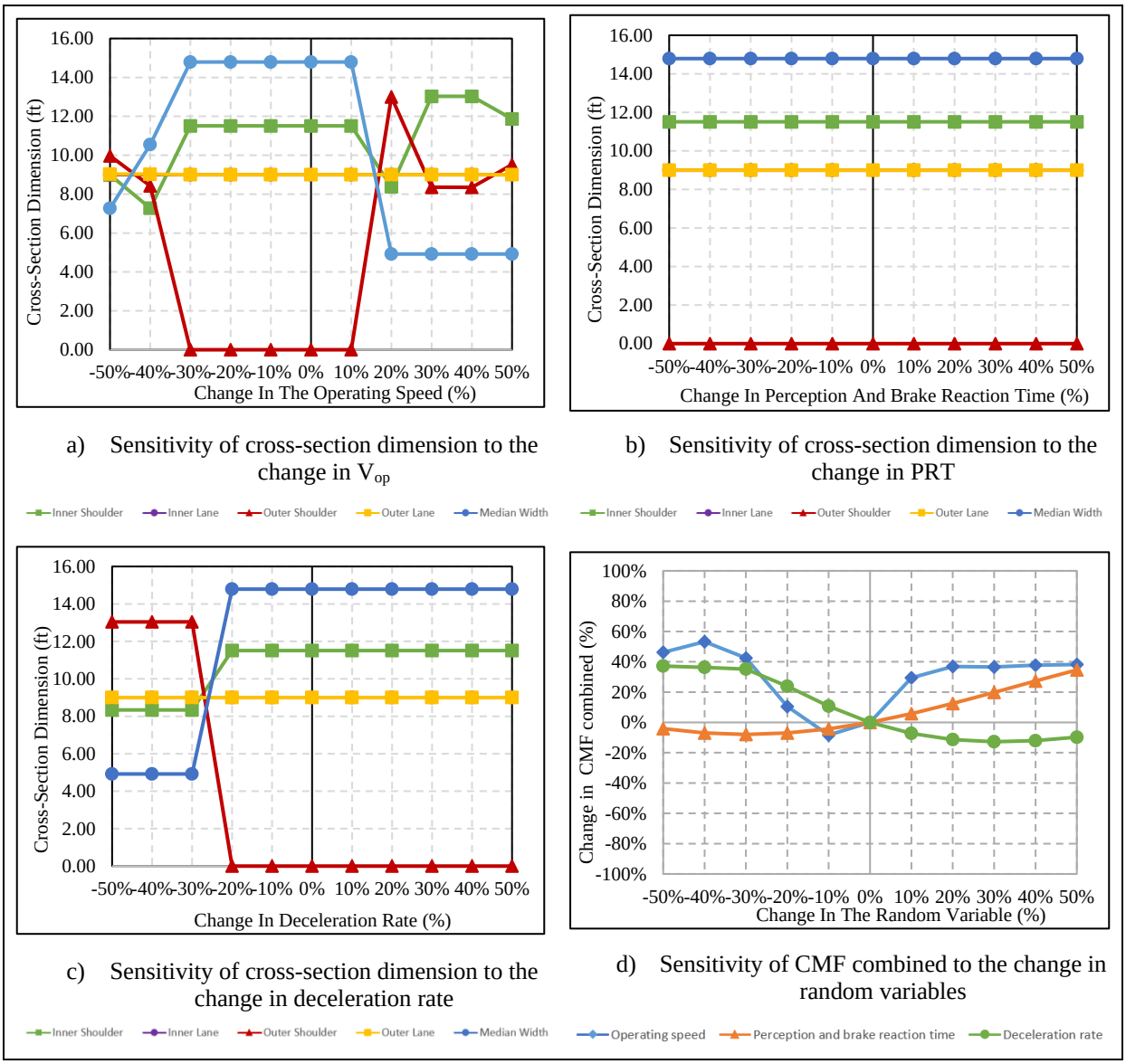

a) Sensitivity of cross-section dimension to the change in V_{op}

b) Sensitivity of cross-section dimension to the change in PRT

c) Sensitivity of cross-section dimension to the change in deceleration rate

d) Sensitivity of CMF combined to the change in random variables

Figure 5.5: Sensitivity analysis for random variables (Curve 2)

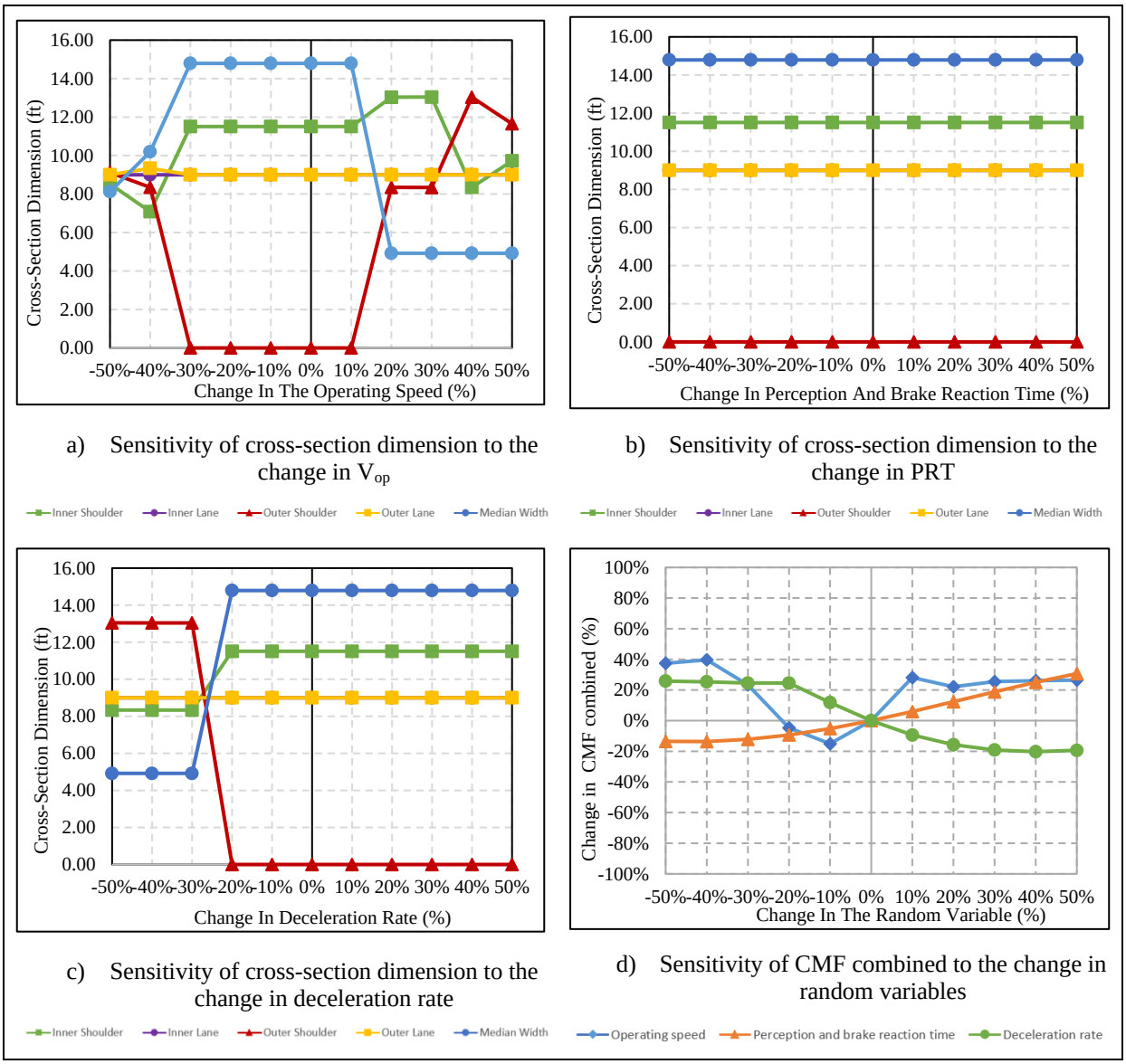

a) Sensitivity of cross-section dimension to the change in V_{op}

b) Sensitivity of cross-section dimension to the change in PRT

c) Sensitivity of cross-section dimension to the change in deceleration rate

d) Sensitivity of CMF combined to the change in random variables

Figure 5.6: Sensitivity analysis for random variables (Curve 3)

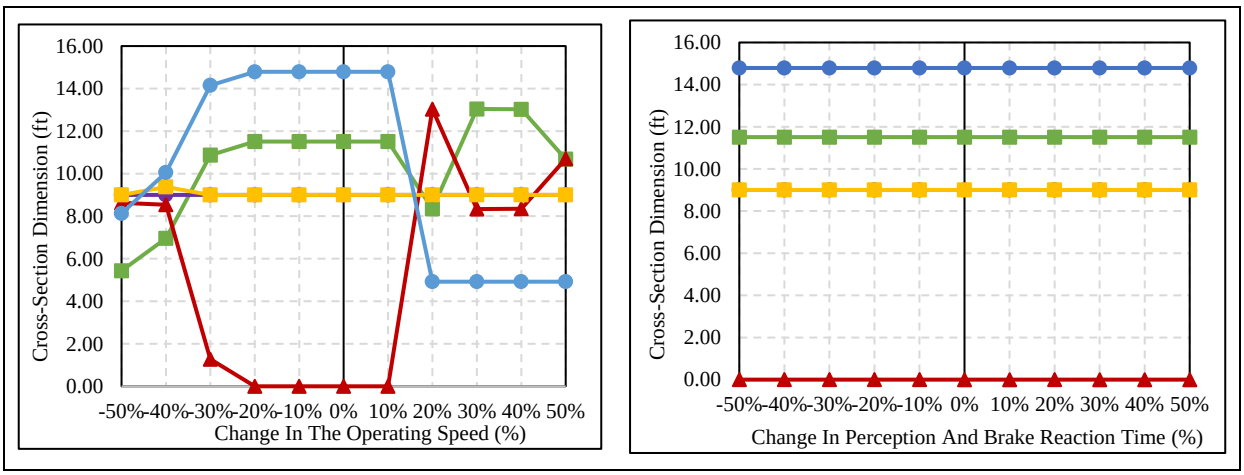

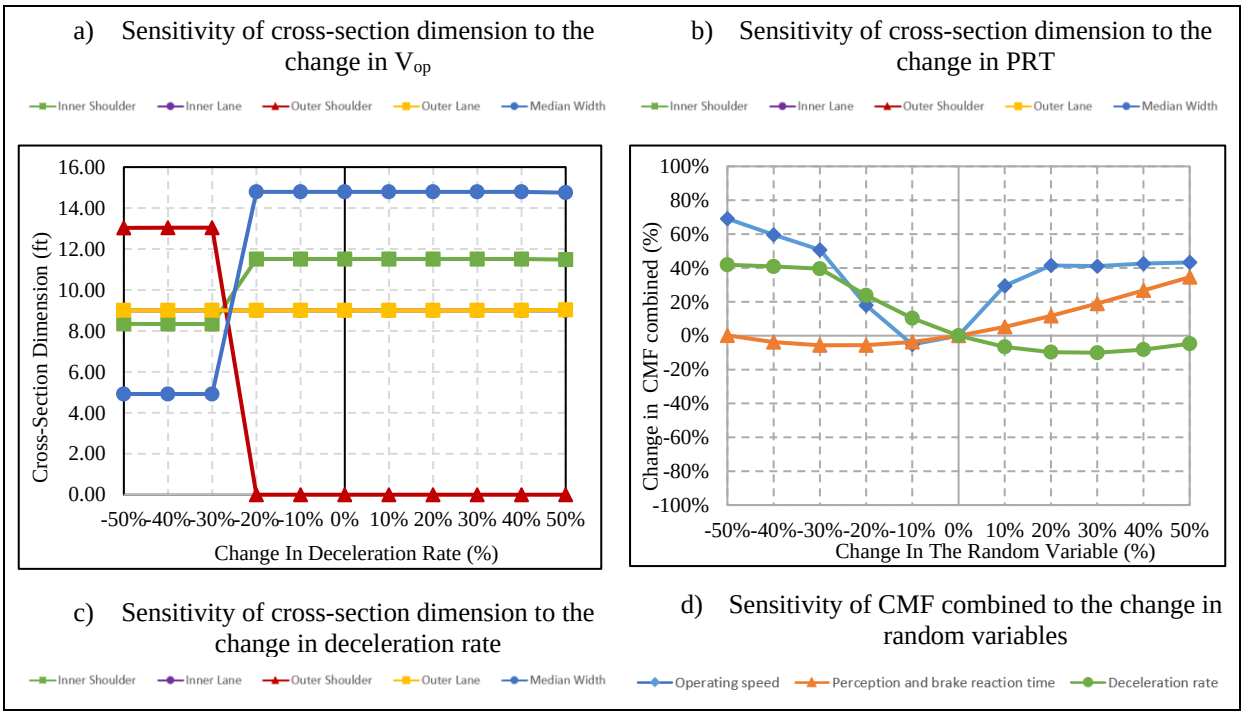

Figure 5.7: Sensitivity analysis for random variables (Curve 4)

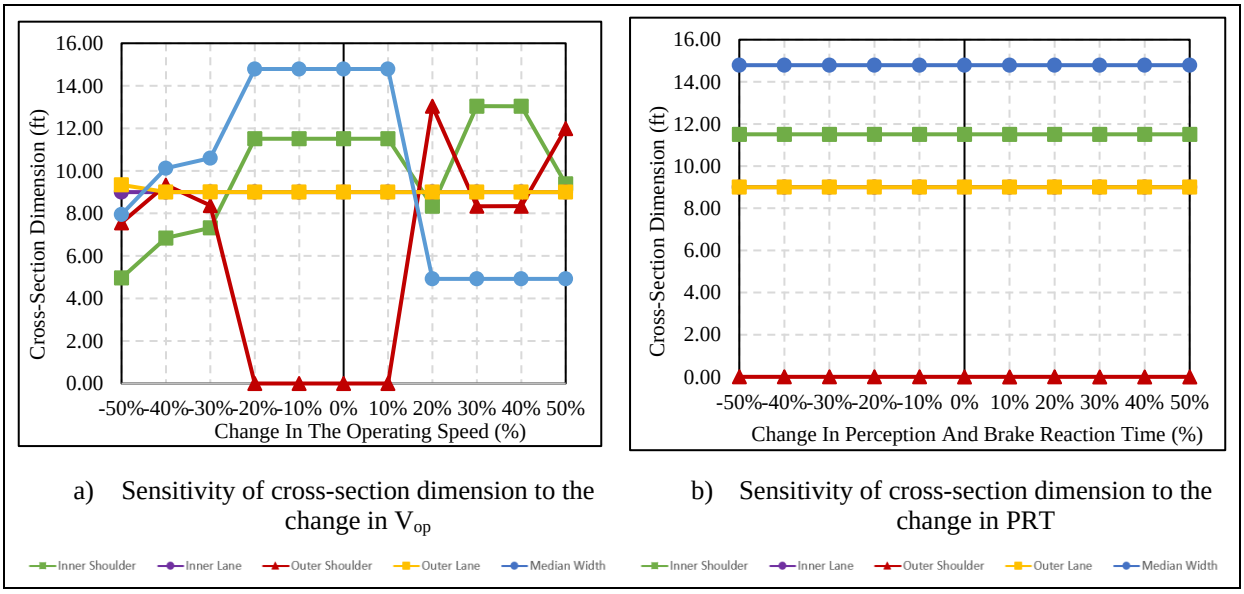

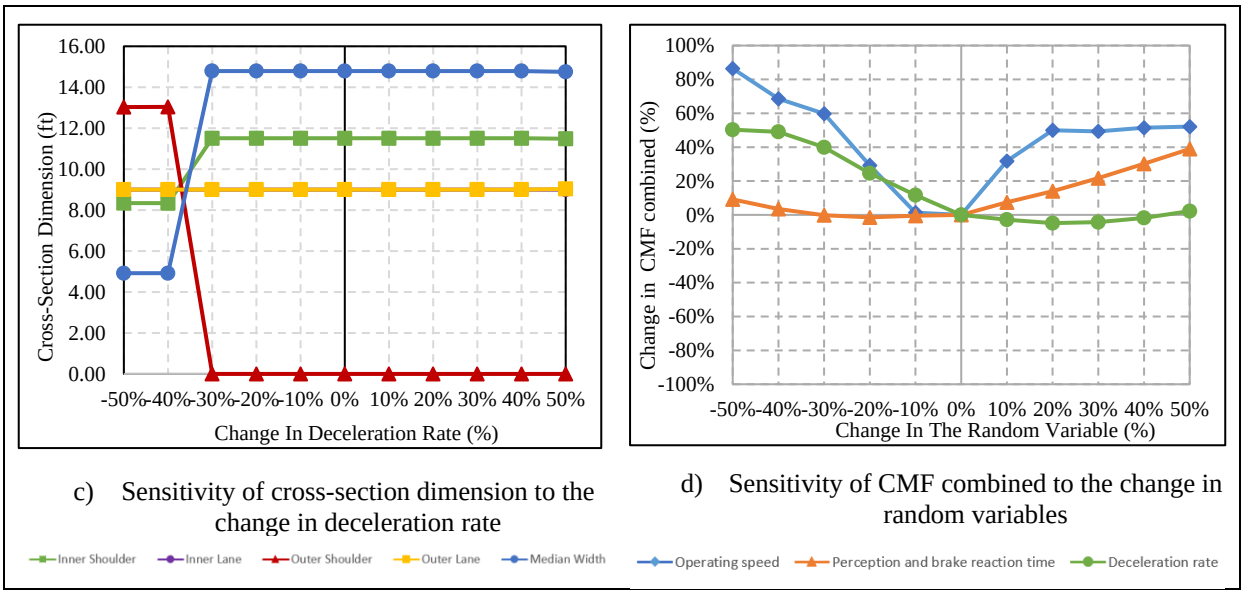

c) Sensitivity of cross-section dimension to the change in deceleration rate

d) Sensitivity of CMF combined to the change in random variables

Figure 5.8: Sensitivity analysis for random variables (Curve 5)